Neocortical Layer-5 tLTD Relies on Non-Ionotropic Presynaptic NMDA Receptor Signaling

Aurore Thomazeau[1,2,*], Sabine Rannio[1,3,*], Jennifer A. Brock[1,3], Hovy Ho-Wai Wong[1,4], P. Jesper Sjöström[1,5]

*) These authors contributed equally.

1) Centre for Research in Neuroscience, Brain Repair and Integrative Neuroscience Program, Departments of Neurology & Neurosurgery and Medicine, The Research Institute of the McGill University Health Centre, Montreal General Hospital, Montreal Quebec, H3G 1A4, Canada

2) Université Côte d'Azur, CNRS UMR7275, Institute of Molecular and Cellular Pharmacology, 06560 Valbonne, France

3) Integrated Program in Neuroscience, McGill University, 3801 University Street, Montreal, Quebec H3A 2B4, Canada

4) Gerald Choa Neuroscience Institute & School of Biomedical Sciences, The Chinese University of Hong Kong, Hong Kong, China

5) Correspondence: jesper.sjostrom@mcgill.ca

Address for editorial correspondence:
Prof P J Sjöström
Centre for Research in Neuroscience
Department of Neurology and Neurosurgery
The Research Institute of the McGill University Health Centre
Montreal General Hospital
1650 Cedar Ave, room L7-225
Montreal Quebec H3G 1A4, Canada
Office: +1-514-934-1934, ext. 44561
Mob: +1-438-826-1971
FAX: +1-514-934-8216

Abstract

In the textbook view, NMDA receptors (NMDARs) act as coincidence detectors in Hebbian plasticity by fluxing Ca^{2+} when simultaneously depolarized and glutamate bound. Hebbian coincidence detection requires that NMDARs be located postsynaptically, but enigmatic presynaptic NMDARs (preNMDARs) also exist. It is known that preNMDARs regulate neurotransmitter release, but precisely how remains poorly understood. Emerging evidence suggest that NMDARs can also signal non-ionotropically, without the need for Ca^{2+} flux. At synapses between developing visual cortex layer-5 (L5) pyramidal cells (PCs), preNMDARs rely on Mg^{2+} and Rab3-interacting molecule 1αβ (RIM1αβ) to regulate evoked release during periods of high-frequency firing, but they signal non-ionotropically via c-Jun N-terminal kinase 2 (JNK2) to regulate spontaneous release regardless of frequency. At the same synapses, timing-dependent long-term depression (tLTD) depends on preNMDARs but not on frequency. We therefore tested if tLTD relies on non-ionotropic preNMDAR signaling. We found that tLTD at L5 PC→PC synapses was abolished by pre- but not postsynaptic NMDAR deletion, cementing the view that tLTD requires preNMDARs. In agreement with non-ionotropic NMDAR signaling, tLTD prevailed after channel pore blockade with MK-801, unlike tLTP. Homozygous RIM1αβ deletion did not affect tLTD, but wash-in of the JNK2 blocker SP600125 abolished tLTD. Consistent with a presynaptic need for JNK2, a peptide blocking the interaction between JNK2 and Syntaxin-1a (STX1a) abolished tLTD if loaded pre- but not postsynaptically, regardless of frequency. Finally, low-frequency tLTD was not blocked by the channel pore blocker MK-801, nor by 7-CK, a non-competitive NMDAR antagonist at the co-agonist site. We conclude that neocortical L5 PC→PC tLTD relies on non-ionotropic preNMDAR signaling via JNK2/STX1a. Our study brings closure to long-standing controversy surrounding preNMDARs and highlights how the textbook view of NMDARs as ionotropic coincidence detectors in plasticity needs to be reassessed.

Keywords

Long-term plasticity, STDP, LTD, LTP, NMDAR, unconventional NMDAR signaling

Introduction

Synapses continuously remodel in response to neuronal activity. Such synaptic plasticity is thought to underlie information storage (Bliss and Collingridge, 1993; Malenka and Bear, 2004; Nabavi et al., 2014) as well as developmental circuit refinement (Cline, 1998; Katz and Shatz, 1996; Song and Abbott, 2001), an idea often attributed to Donald Hebb (1949). More recent work tend to emphasize the role of temporal ordering of activity in determining plasticity, a notion called spike timing-dependent plasticity (STDP) (Markram et al., 2012).

In the STDP paradigm, coincident firing in the range of tens of milliseconds results in long-lasting changes in synaptic efficacy (Feldman, 2012). In classic STDP studies (Bi and Poo, 1998; Feldman, 2000; Markram et al., 1997; Zhang et al., 1998), presynaptic spikes leading postsynaptic spikes by a few milliseconds drive timing-dependent long-term potentiation (tLTP), whereas the opposite temporal ordering elicits timing-dependent long-term depression (tLTD). However, STDP is quite diverse, with rules and mechanisms depending on factors such as synapse type, developmental stage, and neuromodulation (Debanne and Inglebert, 2023; Larsen and Sjöström, 2015; McFarlan et al., 2023).

Many forms of STDP critically depend on NMDARs, which are a subfamily of glutamatergic receptors known for forming heterotetrameric ligand-gated ion channels (Paoletti et al., 2013; Wong et al., 2021). In the case of cortical tLTP, the role of NMDARs is well understood. Action potentials initiated at the soma are thought to backpropagate through dendrites (Stuart and Sakmann, 1994) to elicit nonlinear calcium signals localized to dendritic spines (Koester and Sakmann, 1998) by activating glutamate-bound NMDARs in the postsynapse (Yuste and Denk, 1995). These NMDARs are thus able to act as classic detectors of coincident EPSPs and action potentials in postsynaptic neurons (Markram et al., 1997) because of their dual need for presynaptically released glutamate as well as postsynaptic depolarization to relieve the Mg^{2+} blockade and flux the Ca^{2+} that triggers tLTP (Sjöström and Nelson, 2002; Wong et al., 2021).

In cortical tLTD, however, the role of NMDARs is not as well understood. We previously found evidence that, at L5 PC→PC connections, tLTD relies on preNMDAR signaling (Sjöström et al., 2003, 2007), but precisely how was not clear (Duguid and Sjöström, 2006). After all, the presynaptic spike is long gone by the time preNMDARs bind the released glutamate, arguing

that another presynaptic spike must arrive soon enough to depolarize and unblock glutamate-bound preNMDARs, suggesting a need for high-frequency spiking (Duguid and Sjöström, 2006). Yet tLTD is readily induced at low frequencies (Sjöström et al., 2003).

More recently, we found that preNMDARs differentially regulate evoked and spontaneous release via RIM1aß and JNK2, respectively (Abrahamsson et al., 2017). Interestingly, the JNK-mediated regulation of spontaneous release by preNMDARs was not Mg^{2+}-sensitive (Abrahamsson et al., 2017), revealing the existence of an unconventional form of non-ionotropic NMDAR signaling in the axon (Bouvier et al., 2018; Dore et al., 2017; Wong et al., 2021). If tLTD relied on such non-ionotropic preNMDAR signaling, it would explain why it can be induced at both low and high frequencies, since in this signaling mode, preNMDARs are sensitive to glutamate but not to Mg^{2+} or membrane potential.

Here, we explored how NMDARs signal in tLTD. We found that, regardless of frequency, L5 PC→PC tLTD relies on the non-ionotropic preNMDAR signaling pathway mediated by JNK2, which helps to resolve the long-standing enigma surrounding its lack of frequency dependence (Duguid and Sjöström, 2006).

Results

tLTD relies on presynaptically located NMDARs

We previously reported pharmacological and imaging evidence for preNMDARs at L5 PC→PC synapses that are necessary for neocortical tLTD (Abrahamsson et al., 2017; Buchanan et al., 2012; Sjöström et al., 2003, 2007), but their existence has been disputed (Christie and Jahr, 2009). We therefore wanted to directly challenge our previous findings by sparsely deleting the obligatory GluN1 NMDAR subunit (see Methods) and then measuring tLTD at synaptically connected L5 PC→PC pairs that lacked NMDARs pre- or postsynaptically.

With this approach, we found that preNMDAR deletion abolished high-frequency (HF) tLTD at 20 Hz (see Methods), whereas postsynaptic NMDAR (postNMDARs) deletion did not (**Figure 1**). We previously found that tLTD is expressed presynaptically (Sjöström et al., 2003, 2007). We relied on coefficient of variation (CV) analysis (Brock et al., 2020) to verify that postNMDAR deletion did not alter this (**Figure 1E**). We concluded that L5 PC→PC tLTD relied on pre- but not postNMDARs.

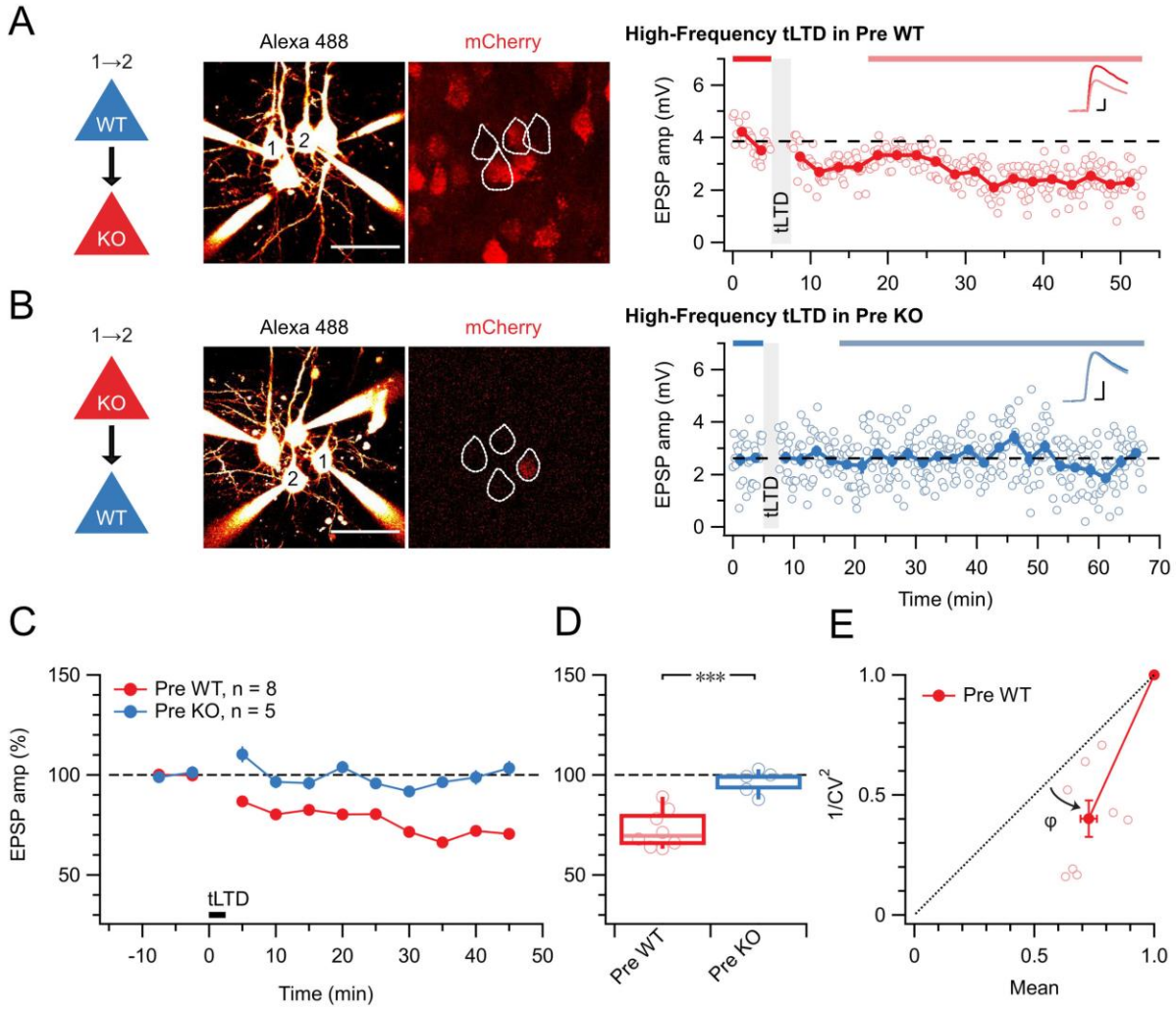

Figure 1. tLTD requires presynaptic NMDARs.

(A) Sample quadruple recording with L5 PCs visualized with Alexa 488 (left, scale bar 50 µm) and NMDAR deletion indicated by mCherry (right). In this wildtype (WT) →KO sample, high-frequency (HF) tLTD at 20 Hz (see Methods) was intact (after/before = 68%, p <0.001), suggesting postNMDARs were not required. Traces (right) were averaged over periods indicated by blue lines. Scale bars: 5 ms, 1 mV.

(**B**) For this KO→WT sample, however, the same induction elicited no plasticity (after/before = 100%, p = 0.99), suggesting tLTD needed preNMDARs. Scale bars as in A.

(C, D) HF tLTD was robustly evoked for presynaptic WT (Pre WT, blue) but not presynaptic KO pairs (Pre KO, red), verifying the need for preNMDARs in tLTD that we previously demonstrated (Sjöström et al., 2003, 2007). Pre WT: WT→WT and WT→KO pooled. Pre KO: KO→WT and KO→KO pooled.

(E) CV analysis indicated that tLTD was presynaptically expressed (φ = 19º ± 4º, n = 8, one-sample *t*-test vs. diagonal, p < 0.001), in agreement with our prior studies (Sjöström et al., 2003, 2007).

Throughout this study, boxplots show medians and quartiles, with whiskers denoting extremes, but data is reported as mean ± SEM, with n indicating number of connections.

tLTD does not rely on ionotropic NMDAR signaling

We previously imaged preNMDAR-mediated Ca^{2+} supralinearities in axons (Abrahamsson et al., 2017; Buchanan et al., 2012). We also found that Mg^{2+}-sensitive ionotropically signaling preNMDARs boost neurotransmitter release during periods of high-frequency activity at L5 PC→PC synapses and that this frequency dependence is inherited from the Mg^{2+} blockade of the preNMDAR channel (Abrahamsson et al., 2017; Wong et al., 2024). Since tLTD is not frequency dependent (Sjöström et al., 2003), we hypothesized that tLTD is not sensitive to blockade of the NMDAR channel pore. To test this hypothesis, we relied on the NMDAR pore blocker MK-801 (Song et al., 2018).

We first wanted to establish a positive control. MK-801 is known to block hippocampal LTP (Nabavi et al., 2013) as well as tLTP at excitatory inputs onto neocortical L2/3 PCs (Bender et al., 2006; Nevian and Sakmann, 2006; Rodríguez-Moreno et al., 2011). At L5 PC→PC synapses, tLTP relies on different NMDARs than tLTD (Sjöström et al., 2003), but the MK-801 sensitivity has to our knowledge not been explored. Here, we found that MK-801 wash-in abolished potentiation (**Figure 2**), suggesting that L5 PC→PC tLTP relies on ionotropically signaling postNMDARs, like tLTP at other neocortical synapses (Bender et al., 2006; Nevian and Sakmann, 2006). We also verified that MK-801 wash-in had no effect on baseline responses elicited at low frequency (**Supplementary Figure 1**), as expected (Abrahamsson et al., 2017; Buchanan et al., 2012; Sjöström et al., 2003; Wong et al., 2024).

With this positive control established, we next explored if L5 PC→PC tLTD and tLTP were equally sensitive to MK-801. However, MK-801 had no effect on tLTD (**Figure 3**). Since the action of MK-801 is activity and voltage dependent (Huettner and Bean, 1988), we were concerned that HF tLTD and low-frequency (LF) tLTD (see Methods) might be differentially affected by this drug, but we found no difference (**Figure 3**).

Even with the positive tLTP control (**Figure 2**), we were concerned that the absence of effect of MK-801 on tLTD was a negative result (**Figure 3**). We therefore wished to strengthen our findings by complementing them with another approach. We thus attempted to block tLTD using 7-chlorokynurenate (7-CK), a co-agonist site blocker that abolishes NMDAR currents (Nabavi et al., 2013) without hindering glutamate binding (Kemp et al., 1988). In control experiments, we found that 7-CK suppressed synaptic responses (**Supplementary Figure 2**) in a

manner consistent with its known additional action as a competitive inhibitor of L-glutamate transport into synaptic vesicles (Bartlett et al., 1998). We therefore waited for synaptic responses to stabilize before inducing tLTD in 7-CK. With this approach, we found that 7-CK was unable to block tLTD (**Figure 4**).

A parsimonious interpretation of these experiments is that tLTP but not tLTD requires ionotropic NMDAR signaling. This interpretation additionally helps to explain why tLTD is not frequency dependent (Sjöström et al., 2003).

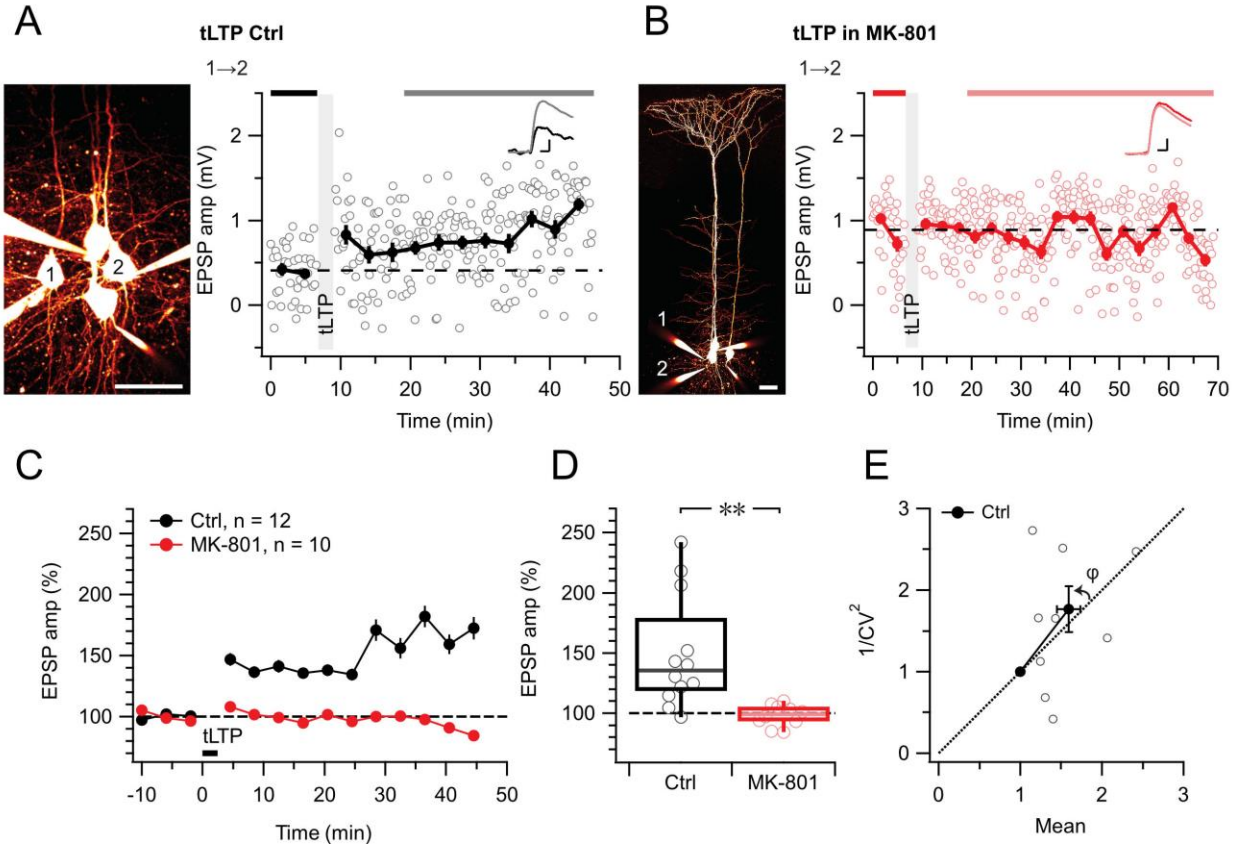

Figure 2. tLTP requires ionotropic NMDAR signaling.

(A) At this sample connection (PC 1→2, see Alexa 594 fills at left, scale bar: 50 µm), tLTP induction was successful (after/before = 210%, $p < 0.001$). Traces (right) were averaged over time periods indicated in black/grey. To avoid MK-801 affecting short-term depression (Abrahamsson et al., 2017; Sjöström et al., 2003), baseline spiking was 0.1 Hz. Scale bars: 5 ms, 0.2 mV.

(B) In this sample, MK-801 abolished tLTP with the same induction protocol (after/before = 95.44%, $p = 0.55$). Baseline spiking and scale bars as in (A).

(C, D) Ensemble data revealed that tLTP was robustly expressed in controls (black) but abolished in MK-801 (red).

(E) CV analysis indicated that tLTP expressed both pre- and postsynaptically to varying degrees across different pairs (φ = 11° ± 15°, n = 10, p =0.44, two data points without potentiation were excluded, see Methods), in agreement with our prior work (Sjöström et al., 2007).

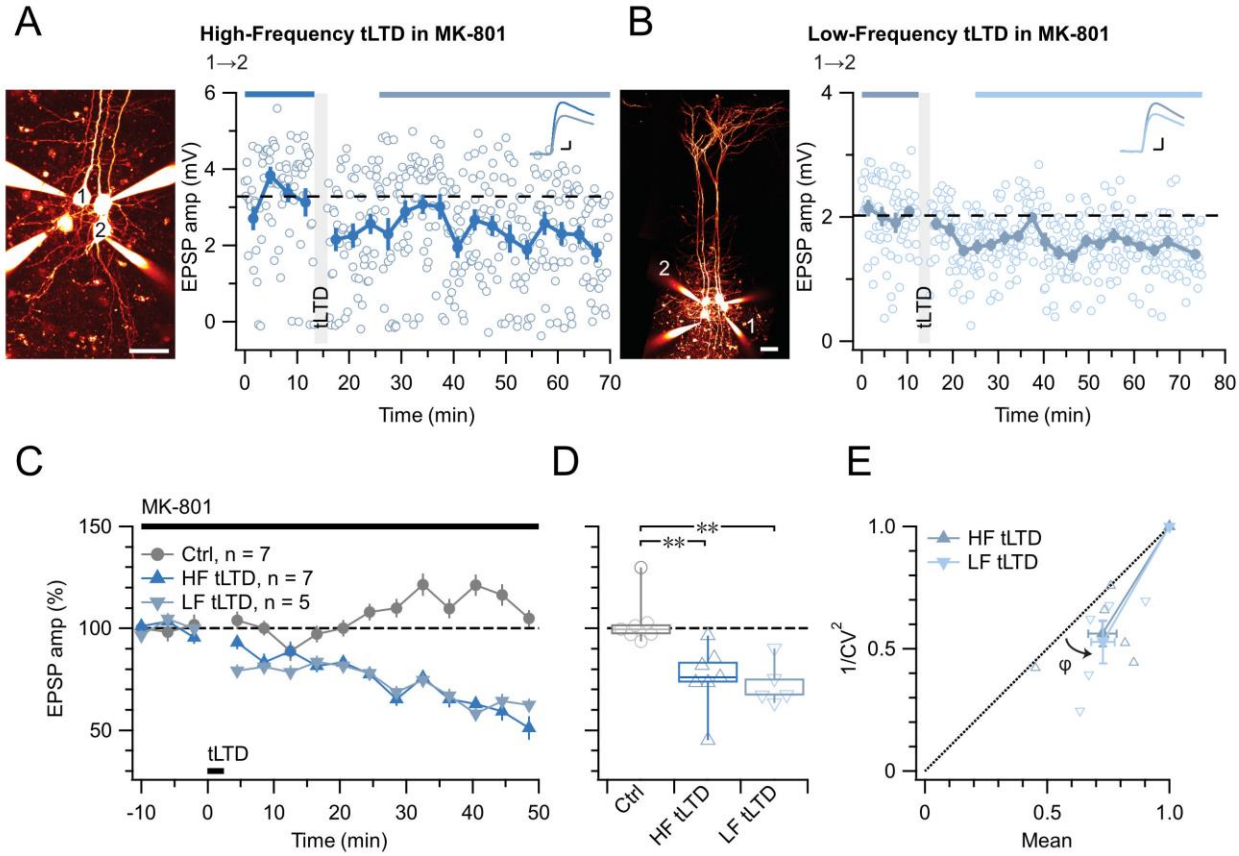

Figure 3. tLTD does not require ionotropic NMDAR signaling.

(A) At this sample connection (PC 1→2, see Alexa 594 fills left, scale bar: 50 µm), HF tLTD was successfully induced in the presence of MK-801 (after/before = 74%, p < 0.001). Traces were averaged over time periods indicated in blue/light blue. Baseline spiking was 0.1 Hz. Scale bars: 5 ms, 0.5 mV.

(B) In this sample, low-frequency (LF) tLTD at 1 Hz (see Methods) was successful in MK-801 (after/before = 78%, p < 0.001). Baseline spiking and scale bars as in A.

(C, D) Ensembles revealed robust tLTD at both low and high frequencies in MK-801 (blue triangles) compared to no-induction MK-801 controls (grey, Welch ANOVA p < 0.01), suggesting that tLTD does not rely on ionotropic NMDAR signaling.

(E) CV analysis indicated that tLTD at both induction frequencies was presynaptically expressed (HF LTD: φ = 13º ± 5º, n = 6, p < 0.05; LF LTD: 15º ± 4º, n = 5, p <0.05), in agreement with our prior findings (**Figure 1**) (Sjöström et al., 2003, 2007). One experiment with <5% plasticity was excluded, see Methods.

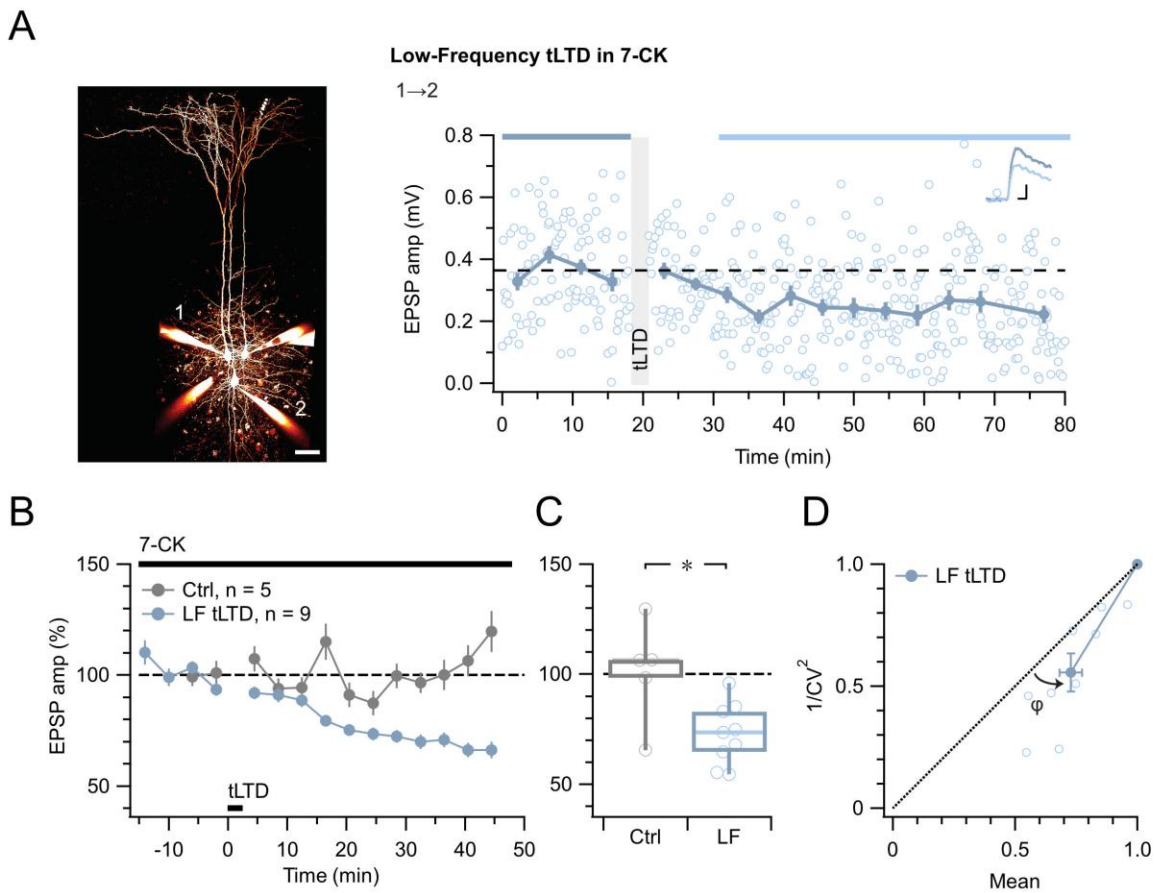

Figure 4. tLTD does not require ligand binding at NMDAR co-agonist site.

(A) At this sample connection (PC 1→2, see Alexa 594 fills at left, scale bar 50 µm), LF tLTD at 1 Hz (see Methods) persisted in the presence of 7-CK (after/before = 68 %, $p < 0.001$). Traces were averaged over time periods indicated in blue/light blue. Baseline spiking was 0.1 Hz. Scale bars: 5 ms, 0.1 mV.

(B, C) Ensemble revealed that LF tLTD persisted in 7-CK (blue) compared to no-induction 7-CK controls (grey), verifying that it does not require ionotropic NMDAR signaling.

(D) CV analysis verified that LF tLTD was presynaptically expressed ($\varphi = 14^{o} \pm 3^{o}$, n = 9, $p < 0.01$), in agreement with our prior findings (**Figure 1**, **Figure 3E**) (Sjöström et al., 2003, 2007).

tLTD relies on JNK2 but not on RIM1αβ

We previously found that ionotropic preNMDAR-mediated regulation of evoked release at L5 PC→PC synapses relies on RIM1αβ (Abrahamsson et al., 2017). Additionally, RIM1α is required for endocannabinoid-mediated LTD in hippocampus (Castillo et al., 2002; Chevaleyre et al., 2007) as well as for LTP in amygdala (Fourcaudot et al., 2008). We therefore explored if

RIM1αβ signaling similarly contributed to L5 PC→PC tLTD, by conditionally deleting RIM1αβ in excitatory neurons (see Methods and Abrahamsson et al., 2017).

We found that L5 PC→PC tLTD was robust in Emx1$^{Cre/+}$;RIM1αβ$^{fl/fl}$ animals (**Figure 5C-E**). The magnitude of tLTD in Emx1$^{Cre/+}$;RIM1αβ$^{fl/fl}$ mice was furthermore indistinguishable to that in WT mice (**Figure 5C, D**). To explore the locus of expression of tLTD, we analyzed paired-pulse ratio (PPR) and CV, which both suggested a presynaptic site of expression (**Figure 5E, F**), like we found before (**Figures 1**, **3E**, **4D**) (Sjöström et al., 2003, 2007). Homozygous RIM1αβ deletion thus had no detectable effect on L5 PC→PC tLTD.

Since we previously found that non-ionotropic preNMDAR signaling requires JNK2 to control spontaneous release (Abrahamsson et al., 2017), we were curious to test the potential need for JNK2 in tLTD. We blocked JNK2 signaling by pre-incubating (see Methods) with the specific inhibitor SP600125 (Bennett et al., 2001), which abolished tLTD (**Figure 5B-E**). Taken together, our results show that tLTD relies on JNK2 but not on RIM1αβ.

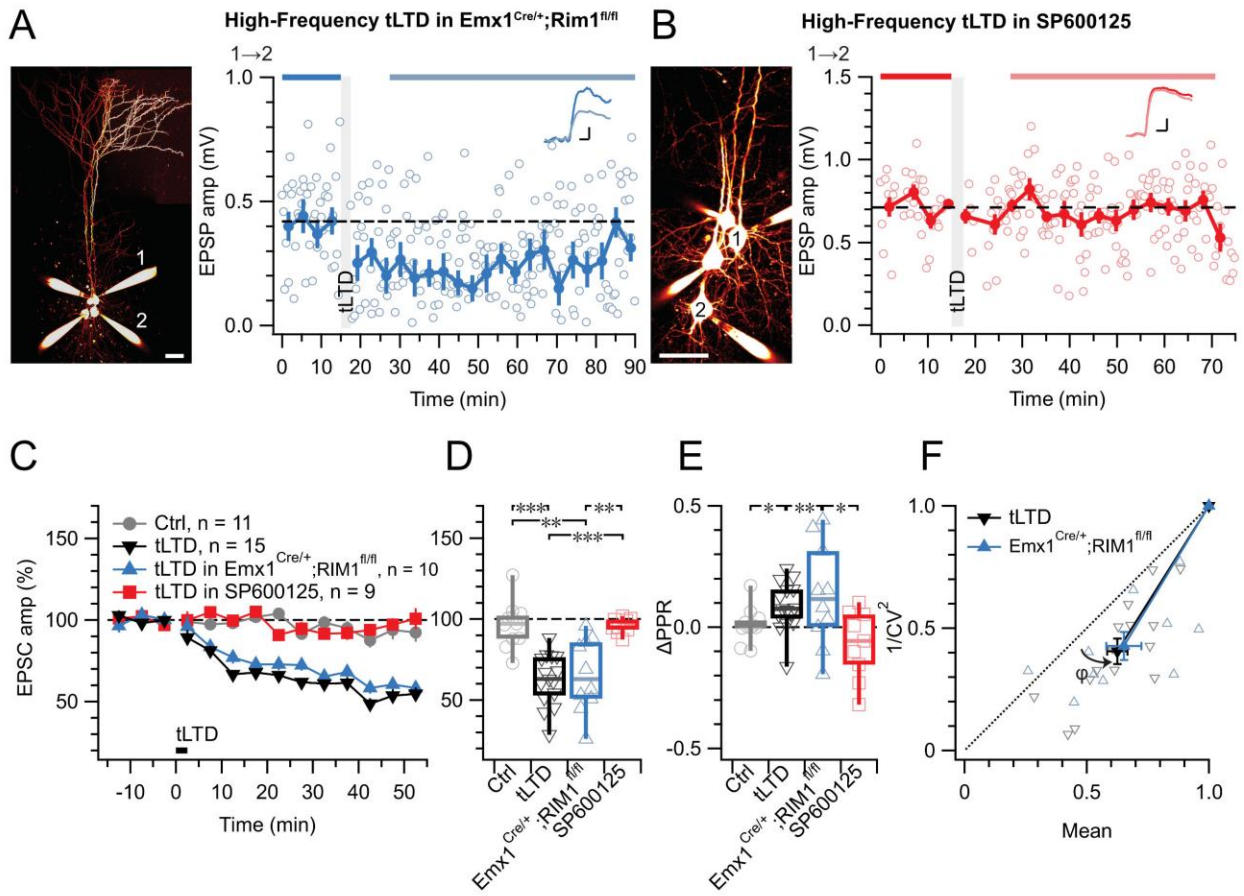

Figure 5. tLTD does not require RIM1αβ but relies on JNK2.

(A) At this sample PC 1→2 connection (left: Alexa 594 fills, scale bar 50 µm) in an acute slice from a homozygous RIM1αβ deletion mouse, tLTD persisted (after/before = 59%, $p < 0.001$). Scale bars: 5 ms, 0.1 mV.

(B) For this sample connection, the JNK2-blocker SP600125 (Bennett et al., 2001) abolished tLTD (after/before = 99%, $p = 0.86$). Scale bars: 5 ms, 0.2 mV.

(C, D) Ensemble data revealed that tLTD after homozygous RIM1αβ deletion (blue) was indistinguishable from WT tLTD (black), thereby dissociating tLTD from RIM1αβ. However, SP600125 robustly disrupted tLTD (red), with an outcome indistinguishable from no-induction controls (grey). Welch ANOVA $p < 0.001$.

(E) tLTD increased PPR (black and blue) compared to controls (grey), suggesting presynaptic expression. Welch ANOVA $p < 0.05$.

(F) CV analysis indicated that tLTD was presynaptically expressed, whether RIM1αβ was deleted ($\varphi = 16^{o} \pm 4^{o}$, $n = 10$, $p < 0.01$) or not ($\varphi = 13^{o} \pm 2^{o}$, $n = 15$, $p < 0.001$), in agreement with our prior findings (**Figure 1**, **Figure 3E**, **Figure 4D**) (Sjöström et al., 2003, 2007).

tLTD relies on presynaptic JNK2 signaling regardless of frequency

To selectively disrupt JNK2/STX1a interactions and associated signaling, we loaded a cell-impermeable variant of the JGRi1 peptide (Marcelli et al., 2019) into pre- or postsynaptic PCs

via the patch pipettes. When loaded presynaptically, HF tLTD was abolished, whereas when loaded postsynaptically, HF tLTD could be induced (**Figure 6A-D**). As before, tLTD was expressed presynaptically (**Figure 6E, F**). This suggested that tLTD was mediated by preNMDAR signaling via the JNK2/STX1a complex.

By comparison with preNMDAR regulation of spontaneous release via JNK2 — which was independent of Mg^{2+} and frequency (Abrahamsson et al., 2017) — this also suggested that the JGRi1 peptide ought to block tLTD at any frequency. We therefore repeated these JGRi1 peptide loading experiments for LF tLTD. As for HF tLTD, when the peptide was loaded presynaptically, LF tLTD was abolished, whereas when loaded postsynaptically, LF tLTD was expressed by presynaptic downregulation of release (**Figure 6G-L**). We note that at low frequency, preNMDARs remained blocked by Mg^{2+} (Abrahamsson et al., 2017; Wong et al., 2024), so this outcome lends further support to the view that tLTD requires non-ionotropic signaling. The sensitivity to pre- but not postsynaptic peptide further cements the view that this form of NMDAR signaling is located presynaptically.

Taken together, these results demonstrate that, regardless of induction frequency, tLTD is mediated by non-ionotropic preNMDAR signaling via the JNK2/STX1a complex in presynaptic neurons.

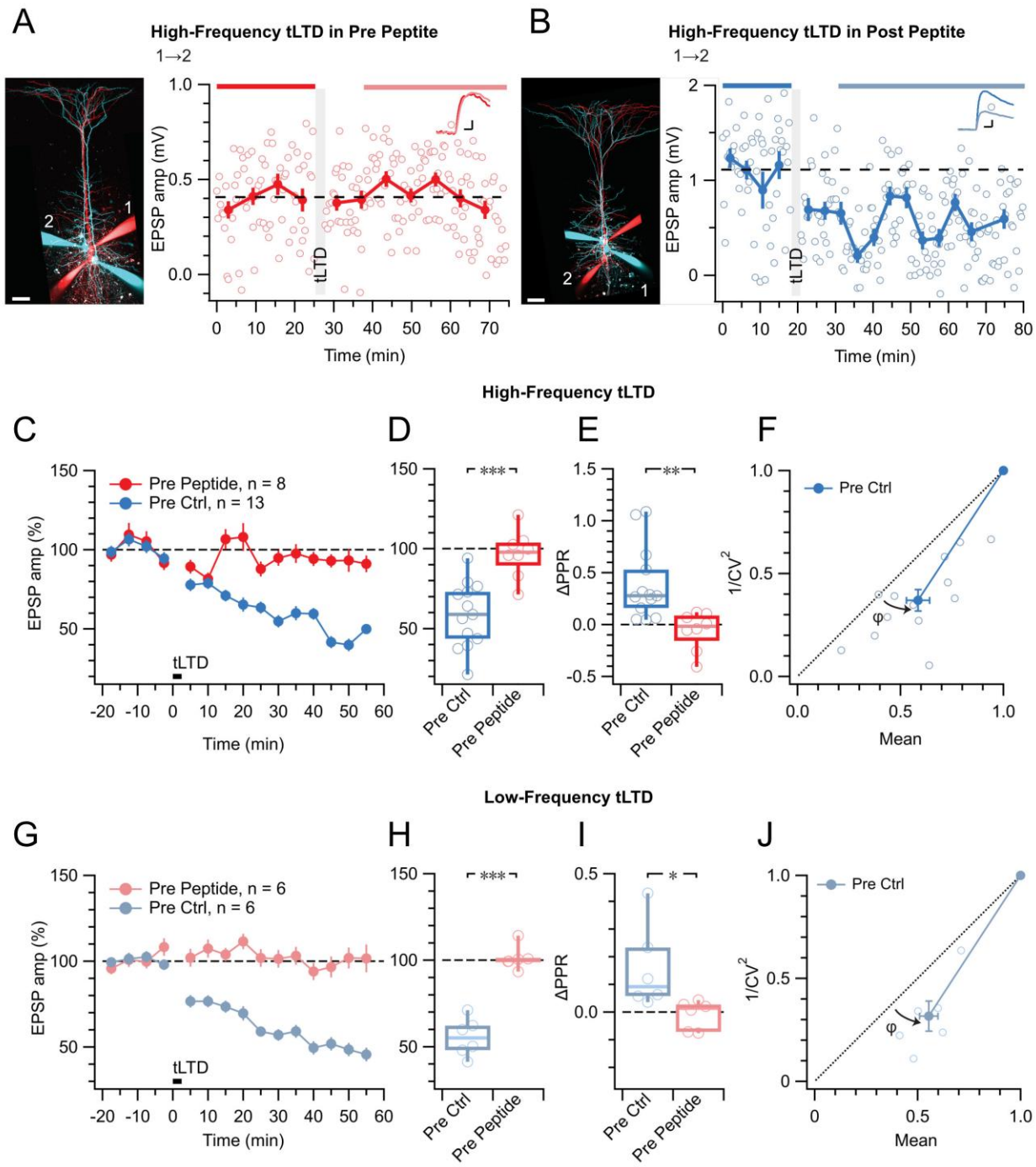

Figure 6. tLTD relies on presynaptic JNK2/STX1 signaling.

(A) Presynaptic loading of peptide disrupting JNK2/STX1 interactions (Marcelli et al., 2019) in this PC 1→2 pair abolished HF tLTD (after/before = 105%, p =0.52). Red cells were loaded with peptide, whereas blue cells were not. Traces were averaged over time periods indicated in red/pink. Scale bar 50 µm, inset scale bars 5 ms, 0.1 mV.

(B) Postsynaptic peptide loading in this PC 1→2 pair had no effect on HF tLTD (after/before = 47%, p <0.001). Inset scale bars 5 ms, 0.2 mV.

(C, D) Presynaptic (red) but not postsynaptic/no peptide loading (blue) abolished HF tLTD, demonstrating a need for presynaptic JNK2/STX1 signaling.

(E) Without presynaptic peptide (blue), HF tLTD induction increased PPR as expected from reduced release, whereas with presynaptic peptide (red), PPR expectedly remained unaffected.

(F) CV analysis of HF tLTD with no presynaptic peptide agreed with presynaptic expression ($\varphi = 13^{o} \pm 3^{o}$, $n = 13$, $p < 0.001$).

(G, H) Presynaptic (red) but not postsynaptic/no peptide loading (blue) abolished LF tLTD, demonstrating that the need for presynaptic JNK2/STX1 signaling was not frequency dependent like ionotropic preNMDAR signaling is (Abrahamsson et al., 2017).

(I) Without presynaptic peptide (blue), LF tLTD induction increased PPR in keeping with presynaptic expression, but with presynaptic peptide (red), PPR was unaffected.

(J) CV analysis of LF tLTD with no presynaptic peptide agreed that release was reduced ($\varphi = 11^{o} \pm 2^{o}$, $n = 6$, $p < 0.01$).

Discussion

The role of preNMDARs in tLTD has long been enigmatic (Duguid and Sjöström, 2006; Sjöström et al., 2003). Our study provides resolution to this long-standing enigma by showing for the first time that tLTD relies on non-ionotropic preNMDAR signaling via JNK2. Our findings thereby further challenge the traditional view of NMDA receptors as ionotropic coincidence detectors and reveal how non-ionotropic preNMDAR signaling can shape STDP.

Reconciling decades of preNMDAR controversy

Although evidence for preNMDARs have been reported for decades (Aoki et al., 1994; Berretta and Jones, 1996; DeBiasi et al., 1996; Glitsch and Marty, 1999; Liu et al., 1997), this receptor type has been controversial. For instance, one study (Christie and Jahr, 2009) could not find the preNMDARs that we reported as underlying L5 PC→PC tLTD (Sjöström et al., 2003, 2007). Several other studies, however, largely corroborated our findings of preNMDARs at L4 PC → L2/3 PC synapses and elsewhere (Banerjee et al., 2014; Banerjee et al., 2009; Bender et al., 2006; Brasier and Feldman, 2008; Corlew et al., 2007; Rodríguez-Moreno and Paulsen, 2008). Then again, one study argued that the NMDARs that underlie L4 PC → L2/3 PC tLTD are actually postsynaptic (Carter and Jahr, 2016). Similar disagreements exist in cerebellum, with some studies reporting preNMDARs (Casado et al., 2000; Casado et al., 2002; Glitsch and Marty, 1999) and others arguing that they do not exist (Christie and Jahr, 2008).

Central to the preNMDAR controversy has been how they signal. Classically, NMDARs need both glutamate and depolarization to relieve Mg^{2+} blockade, open up, and signal via

calcium flux (Dore et al., 2017; Wong et al., 2021). Consistently, preNMDARs often require high-frequency spike trains to activate (Abrahamsson et al., 2017; Bidoret et al., 2009; Buchanan et al., 2012; McGuinness et al., 2010; Sjöström et al., 2003; Wong et al., 2021), as a single spike that elicits glutamate release is gone by the time preNMDARs bind the glutamate. However, preNMDARs also govern spontaneous release (Abrahamsson et al., 2017; Berretta and Jones, 1996; Buchanan et al., 2012; Kunz et al., 2013; Sjöström et al., 2003) and tLTD (Sjöström et al., 2003), which both occur at low frequencies, leading to a long-standing contradiction in the field (Banerjee et al., 2009; Duguid and Sjöström, 2006; Sjöström et al., 2003).

This controversy can be resolved by several intriguing preNMDAR properties. Whereas postNMDARs are ubiquitously expressed, preNMDARs are only found at specific synapse types (Banerjee et al., 2014; Brasier and Feldman, 2008; Buchanan et al., 2012; Larsen et al., 2014). PreNMDARs are thus easy to miss if different synapse types are mixed experimentally. Furthermore, preNMDARs often rely on particular subunits and conditions that reduce the flux of Ca^{2+} (Banerjee et al., 2009; Kunz et al., 2013; Larsen et al., 2011), leading to weak signals that may be hard to detect.

Finally, preNMDARs can also signal non-ionotropically to control release (Abrahamsson et al., 2017; Wong et al., 2024). If the expectation is that NMDARs can only signal ionotropically, this may confound experimental interpretation. For instance, manipulations such as loading cells internally with MK-801 to block NMDARs from the inside or with BAPTA to chelate Ca^{2+} may become inconclusive. However, non-ionotropic NMDAR signaling has been reported broadly, for instance in classic LTD (Nabavi et al., 2013; Nielsen et al., 2024; Park et al., 2022), structural plasticity (Park et al., 2022; Stein et al., 2021; Thomazeau et al., 2021), and ischemic excitotoxicity (Weilinger et al., 2016), so this mode of NMDAR signaling is not necessarily rare.

In fact, non-ionotropic signaling has also been found for other ionotropic channels, such as kainate receptors (Rodriguez-Moreno and Lerma, 1998), AMPA receptors (Takago et al., 2005; Wang and Durkin, 1995), and even voltage-gated Ca^{2+} channels (Trus and Atlas, 2024). The classic textbook view of receptor types as strictly ionotropic or non-ionotropic is therefore not solidly anchored in the biology.

Our finding that preNMDAR signaling in L5 PC→PC tLTD is non-ionotropic explains why this form of plasticity does not depend on frequency (Duguid and Sjöström, 2006; Sjöström et al., 2003). This is because, in this signaling mode, preNMDARs are sensitive to glutamate but not to Mg^{2+} or membrane potential, so there is no need for spikes to arrive in quick succession to provide the depolarization that would be required for ionotropic preNMDAR signaling (Duguid and Sjöström, 2006).

Overall, our finding that non-ionotropically signaling preNMDARs are key to L5 PC→PC tLTD thus align with much of the prior literature while simultaneously bringing closure to long-standing controversies (Bouvier et al., 2018). Our genetic deletion approach furthermore firmly situate the NMDARs needed for tLTD in the pre- rather than the postsynaptic cell of L5 PC→PC pairs (Carter and Jahr, 2016).

A hitherto unappreciated role for JNK2 in tLTD

JNKs are Serine-Threonine kinases that belong to the mitogen-activated protein kinase family and mediate stress stimuli, e.g., cytokines, ultraviolet irradiation, and heat shock. There are three closely related vertebrate genes: JNK1 and JNK2 are ubiquitous, while JNK3 is primarily neuronal (Yamasaki et al., 2012). In the brain, JNKs are key developmental regulators, for instance of neuronal migration, dendrite formation, and axon maintenance (Yamasaki et al., 2012).

We previously demonstrated that tLTD at L5 PC→PC connections requires simultaneous activation of preNMDARs and endocannabinoid CB1 receptors (Sjöström et al., 2003). It has long been known that JNK is activated by NMDARs (Coffey, 2014; Mukherjee et al., 1999) as well as by CB1 receptors (Rueda et al., 2000). More recently, we and others established that preNMDARs regulate spontaneous release by signaling via JNK2 (Abrahamsson et al., 2017; Nisticò et al., 2015) and that this regulation critically depends on an interaction between JNK2 and STX1a (Marcelli et al., 2019). Interestingly, it was previously proposed that JNK2 signaling is involved in behavioral learning as well as in classical NMDAR-dependent LTD (Curran et al., 2003; Morel et al., 2018). Our study, however, is to our knowledge first to show a need for JNK2 signaling specifically in tLTD, which relies on mechanistic underpinnings that differ from classical LTD, such as retrograde endocannabinoid signaling (Bender et al., 2006; Nevian and Sakmann, 2006; Sjöström et al., 2003). Furthermore, in our hands, the activation of JNK2 is

achieved by non-ionotropic preNMDAR action. Our present study thus extends the prior literature by suggesting that JNK2 signaling may be a general principle that applies to distinct forms of long-term plasticity.

Diverse preNMDAR signaling across different synapse types

In our hands, the NMDAR channel pore blocker MK-801 surprisingly did not block tLTD at L5 PC→PC connections, even though several other studies of tLTD at L4 PC → L2/3 PC synapses reported that MK-801 abolishes tLTD (Banerjee et al., 2014; Larsen et al., 2014; Rodríguez-Moreno et al., 2013; Rodríguez-Moreno et al., 2011; Rodríguez-Moreno and Paulsen, 2008). This difference is likely due to non-ionotropic versus ionotropic preNMDAR tLTD at L5 PC→PC and L4 PC → L2/3 PC synapses, respectively. This mechanistic distinction is generally consistent with the view that STDP depends on synapse type (Larsen and Sjöström, 2015; McFarlan et al., 2023). In fact, tLTD is mediated by distinct mechanisms even for different synaptic input types onto the same L2/3 PCs (Banerjee et al., 2009; Larsen et al., 2014).

A corollary from this synapse-specific difference in non-ionotropic versus ionotropic preNMDAR tLTD at L5 PC→PC and L4 PC → L2/3 PC synapses is a differential frequency dependence. Indeed, at L4 PC → L2/3 PC synapses, a frequency-dependent form of presynaptic self-depression has been reported (Rodríguez-Moreno et al., 2013). Such frequency dependence of tLTD does not, however, exist at L5 PC→PC connections (Sjöström et al., 2003).

Curiously, preNMDARs at L5 PC→PC connections signal ionotropically to boost neurotransmitter release during high-frequency firing (Abrahamsson et al., 2017; Buchanan et al., 2012; Sjöström et al., 2003; Wong et al., 2024). This boosting relies on RIM1αβ (Abrahamsson et al., 2017) and mTOR-mediated protein synthesis in L5 PC axons (Wong et al., 2024), yet is synapse-type-specific, so does not affect L5 PC→interneuron synapses (Buchanan et al., 2012; Wong et al., 2024). Consequently, MK-801 blocks preNMDAR-mediated boosting of evoked L5 PC→PC release (Abrahamsson et al., 2017; Buchanan et al., 2012; Sjöström et al., 2003).

Another corollary from non-ionotropic preNMDAR signaling in tLTD is that removing Mg^{2+} to unblock the channel pore should not induce LTD at L5 PC→PC synapses during low-frequency firing. In agreement, reduced Mg^{2+} does not elicit LTD but actually boosts

neurotransmission (Abrahamsson et al., 2017; Wong et al., 2024). Whether or not Mg^{2+} washout promotes LTD at L4 PC → L2/3 synapses has not been explored, as far as we know.

Caveats

We relied on JNK2 blockade as a proxy for non-ionotropic preNMDAR signaling, as we established this hallmark feature of flux-independent preNMDAR signaling of L5 PCs in a previous study (Abrahamsson et al., 2017). It is, however, presently unclear how well this proxy generalizes. A drug that specifically blocks non-ionotropic but not ionotropic NMDAR signaling would resolve this, much like MK-801 does the vice versa. To our knowledge, such a drug presently does not exist.

As mentioned above, PreNMDAR and CB1 receptor co-activation is required for L5 PC→PC tLTD (Sjöström et al., 2003). Although L5 PC→PC tLTD does not depend on frequency (Sjöström et al., 2003), consistent with the non-ionotropic preNMDAR signaling we provide evidence for here, chemical LTD (cLTD) induced by wash-in of cannabinoid CB1 receptor antagonists is in fact frequency dependent (Sjöström et al., 2003). This apparent discrepancy is difficult to explain, because tLTD requires CB1 receptor signaling at low as well as high frequencies (Sjöström et al., 2003). Although the frequency dependence of cLTD is consistent with its known sensitivity to MK-801 (Sjöström et al., 2003), an apparent disagreement remains. A potential explanation is that CB1 receptor signaling in tLTD is phasic whereas that in cLTD is tonic, and phasic/tonic CB1 signaling paths are known to differ mechanistically (Castillo et al., 2012). To address this, rapid photolysis of caged CB1 receptor agonists (Heinbockel et al., 2005) may mimic tLTD better than slow wash-in of cannabinoid CB1 receptor antagonists (Sjöström et al., 2003). Resolving this enigma will require future work.

NMDAR signaling that does not involve ion flux has sometimes been termed *metabotropic* (e.g., Nabavi et al., 2013). This designation can be confusing, as it could imply G-protein coupling (Heuss and Gerber, 2000), which has not been conclusively demonstrated for NMDARs. We therefore prefer to use the term *non-ionotropic* until future studies reveal if the underlying mechanism is indeed G-protein linked.

Our experiments were conducted in juvenile visual cortex, so caution is warranted when extrapolating our findings to mature circuits, which may rely on different plasticity mechanisms (Banerjee et al., 2009; Corlew et al., 2007; Larsen et al., 2014; Martínez-Gallego et al., 2022).

Further studies in older animals will be important to determine whether the adult brain relies on non-ionotropic preNMDAR signaling in STDP.

Future directions and implications for disease

Our study provides fresh perspective on non-ionotropic function for preNMDARs in tLTD at neocortical synapses. By engaging JNK2-mediated signaling independent of Ca^{2+} influx, preNMDARs contribute to STDP in a manner that has not been previously appreciated. Our findings challenge the traditional view of NMDARs as coincidence detectors in Hebbian plasticity and highlight the diversity of synaptic plasticity mechanisms (Larsen and Sjöström, 2015; McFarlan et al., 2023). Future studies will be needed to explore the broader implications of non-ionotropic NMDAR signaling in other brain regions and under different physiological conditions.

It is crucial to understand how NMDARs operate, as they are hotspots for major synaptic pathologies such as Alzheimer, schizophrenia, and epilepsy (Nugent et al., 2022; Paoletti et al., 2013). For instance, a central hypothesis in schizophrenia research is based on NMDAR hypofunction (Lisman et al., 2008). Yet, if one were to rationally create an NMDAR-based therapy for schizophrenia, one would need to know which type of NMDAR signaling is relevant. Future studies may thus reveal the potential therapeutic relevance of targeting distinct NMDARs signaling pathways.

Methods

Animals and Ethics Statement

The animal study was reviewed and approved by the Montreal General Hospital Facility Animal Care Committee (The MGH FACC) and adhered to the guidelines of the Canadian Council on Animal Care (CCAC). At postnatal day 11 to 18, male or female mice were anaesthetized with isoflurane and sacrificed once the hind-limb withdrawal reflex was lost. Transgenic animals had no abnormal phenotype. Sparse NMDAR deletion was achieved by removing the obligatory GluN1 subunit in a subset of L5 PCs by neonatal injection (Kim et al., 2014) of AAV-eSYN-mCherry-iCre into V1 of $Grin1^{fl/fl}$ mice (a.k.a. $NR1^{flox}$) obtained from The Jackson Laboratory (#005246, see below). A Cre-loxP recombinase strategy (Nagy, 2000) was

used to generate transgenic mice after two generations with RIM1αβ homozygously conditionally deleted in excitatory cells, as genome-wide RIM1αβ knockout impairs survival (Mittelstaedt et al., 2010). Homozygous Emx1$^{Cre/Cre}$ mice (Gorski et al., 2002) were obtained from The Jackson Laboratory (#005628). Homozygous RIM1αβ$^{fl/fl}$ mice (Kaeser et al., 2008) were kindly gifted by Pascal Kaeser (Harvard University, MA). Heterozygous Emx1$^{Cre/+;}$RIM1αβ$^{fl/+}$ mice were generated by crossing Emx1$^{Cre/Cre}$ with RIM1αβ$^{fl/fl}$ mice. Emx1$^{Cre/+}$;RIM1αβ$^{+/+}$ and RIM1αβ$^{fl/fl}$ mice were generated by crossing Emx1$^{Cre/Cre}$;RIM1αβ$^{fl/+}$ mice with RIM1αβ$^{fl/+}$;no-Cre mice (Abrahamsson et al., 2017). These distributed in a Mendelian fashion and had viability indistinguishable from that of C57BL/6 mice. To determine the genotype of each animal, tail biopsy and tattooing were performed on mice before the age of P6. Genotyping was carried out using standard methodology with Jackson Laboratory primers (RIM1: 12061, 12062; Emx1: oIMR1084, oIMR1085, oIMR4170, oIMR4171) using QIAGEN HotStarTaq DNA Polymerase kit (203203) and dNTPs from Invitrogen/Thermo-Fisher (18427-013) (Abrahamsson et al., 2017). Wildtype (WT) denotes C57BL/6J (Jackson Laboratory #000664), RIM1αβ$^{fl/fl}$;no-Cre and genetically unaffected littermates (Emx1$^{Cre/+}$;RIM1αβ$^{+/+}$).

Viral injections

Cre recombinase was delivered by viral injection of AAV9-eSYN-mCherry-T2A-iCre-WPRE (Vector Biolabs, Cat No. VB4856) into the primary visual cortex of Grin1$^{fl/fl}$ neonates (P0-2) to generate a conditional NMDAR deletion through Cre-loxP recombination at the site of the Grin1 gene. This cuts the Grin1 genetic sequence thus preventing the cell from producing the GluN1 subunit. As the GluN1 subunit is obligate, the cells expressing the virus will not express functional NMDARs. Cells expressing the viral construct were detected via an mCherry tag. Pups were anesthetized by putting them on ice and viral injection was delivered with a needle syringe held in a stereotactic injection setup and connected to a microinjector apparatus. The animal head was held in place with ear bars and the tip of the injection needle was zeroed to lambda. The needle was then positioned to the following coordinates: x = ± 1.10; y = 0.00. The needle was lowered until it reached the pial surface, where the z coordinate was zeroed. Three injections of 0.2-0.3µl each were performed at z1 = -0.20; z2 = -0.15; and z3 = -0.10. Both hemispheres were injected to increase the number of slices available for experiments and to reduce the risk of seeing no expression in an animal on the experimental day, both of which enhanced productivity. The AAV9 serotype has a particularly high tropism for the central

nervous system (Foust et al., 2009) and the enhanced synapsin (eSYN) promoter specifically targets neurons (Hioki et al., 2007). T2A is a self-cleaving peptide and facilitates co-expression of Cre recombinase and mCherry (Liu et al., 2017). Finally, the Woodchuck Hepatitis Virus (WHP) Posttranscriptional Regulatory Element (WPRE) enhances expression levels of the viral-encoded proteins (Klein et al., 2006), allowing successful expression in neocortical neurons, including pyramidal cells. By controlling the viral titer, expression levels were regulated to achieve sparse genetic deletion of NMDARs in primary visual cortex neurons (Kim et al., 2014).

Acute Slice Preparation

After decapitation, the brain was removed and placed in ice-cold (~4°C) artificial cerebrospinal fluid (ACSF), containing in mM: 125 NaCl, 2.5 KCl, 1 $MgCl_2$, 1.25 NaH_2PO_4, 2 $CaCl_2$, 26 $NaHCO_3$ and 25 glucose, bubbled with 95% O_2/5% CO_2. Osmolarity of the ACSF was adjusted to 338 mOsm with glucose. Oblique coronal 300-µm-thick acute brain slices were prepared using a Campden Instruments 5000 mz-2 vibratome (Lafayette Instrument, Lafayette, IN, USA). Brain slices were kept at ~33˚C in oxygenated ACSF for ~15 min and then allowed to cool at room temperature for at least one hour before we started the recordings.

Electrophysiology

Experiments were carried out with ACSF heated to 32-34°C with a resistive inline heater (Scientifica Ltd), with temperature recorded and verified offline. If outside this range, recordings were truncated or not used. Patch pipettes with a resistance of 4-6 MΩ were pulled using a P-1000 electrode puller (Sutter Instruments, Novato, CA, USA) from medium-wall capillaries. Pipettes were filled with K-gluconate internal solution (containing in mM: KCl, 5: K-Gluconate, 115; K-HEPES, 10; MgATP, 4; NaGTP, 0.3; Na-Phosphocreatine, 10; and 0.1% w/v Biocytin, adjusted with KOH to pH 7.2-7.4 and sucrose to osmolality of 310 mOsm (Abrahamsson et al., 2017). 40 µM and 80 µM Alexa Fluor 594 or Alexa Fluor 488 dyes, respectively, was supplemented to internal solution to permit post-hoc analysis of cell morphology with two-photon laser-scanning microscopy (Blackman et al., 2014; Lalanne et al., 2016). Neurons were patched using infrared video Dodt contrast (built in-house with Thorlabs equipment) with an Olympus LUMPlanFL N 40×/0.80 objective on a customized microscope (SliceScope, Scientifica Ltd UK). Primary visual cortex (V1) was distinguished from surrounding V2 based on the presence of cortical layer 4. Pyramidal cells (PCs) in L5 of V1 were targeted based upon

their prominent apical dendrite and large triangular somata. Morphometry and cell identity were verified using 2-photon microscopy of Alexa 594/488 fluorescence. Whole-cell recordings were carried out using BVC-700A amplifiers (Dagan Corporation, Minneapolis, MN). Recordings in current-clamp mode were acquired at 40 kHz with PCI-6229 boards (National Instruments, Austin, TX) using our in-house MultiPatch software (Watanabe et al., 2023) (https://github.com/pj-sjostrom/MultiPatch) running in Igor Pro 7 to 9 (WaveMetrics Inc., Lake Oswego, OR).

Since the rate of connectivity in rodent primary visual cortex among L5 PCs is only 10-15% (Sjöström et al., 2001; Song et al., 2005), quadruple whole-cell recording was employed to enable the simultaneous testing of 12 PC→PC connections (Abrahamsson et al., 2016). GΩ seals were first formed on all four cells followed by rapid successive break-through, to avoid plasticity washout (Lalanne et al., 2016). To identify monosynaptic PC→PC connections in current-clamp mode, five spikes were evoked in each cell at 30 Hz by 5-ms-long current injections of 1.3-nA magnitude, repeated every 20 seconds, and averaged across 10 repetitions. A 250-ms-long test pulse of -25 pA was used to measure input and series resistance. Spike trains in different cells were separated from one another by 700 ms to prevent accidental induction of long-term plasticity (Abrahamsson et al., 2017; Lalanne et al., 2016; Sjöström et al., 2003). If no PC→PC connections were detected, all four recordings were stopped, and another set of four cells were patched with new pipettes, either nearby or in a new acute slice.

In paired recordings, synaptic responses were strictly unitary and subthreshold (Chou et al., 2024; Song et al., 2005), ensuring that inhibitory circuits were not inadvertently recruited. There was therefore no need to pharmacologically block GABAergic transmission.

STDP experiments

We induced tLTD by evoking postsynaptic firing 25 ms before presynaptic firing, either at 20 Hz or at 1 Hz (Sjöström et al., 2001, 2003), which we refer to as HF and LF tLTD, respectively, throughout the present study. tLTP was induced by evoking presynaptic firing 10 ms before postsynaptic cell firing at 50 Hz (Sjöström et al., 2001).

To ensure good signal-to-noise ratio, we only used PC→PC connections >0.3 mV, like before (Sjöström et al., 2007). For Figures 1 through 4, presynaptic cells were spiked once every 10 seconds (see below for clarification). For Figures 5 and 6, presynaptic cells were typically spiked

five times at 30 Hz every 20 seconds during baseline periods, resulting in trains of EPSPs, which we denote $EPSP_1$ through $EPSP_5$. We assessed plasticity by calculating the ratio of $EPSP_1$ amplitude averaged across post-induction and pre-induction periods, as indicated in figures. Synaptic stability was assessed using a *t*-test of Pearson's *r* for $EPSP_1$ across the pre-induction baseline period, with $p < 0.05$ implying instability. Recordings with unstable baseline, > 30% change in input resistance, or > 8 mV change in resting membrane potential were truncated or discarded, like before (Sjöström et al., 2001, 2003, 2007).

To determine the locus of neocortical STDP expression, analysis of the coefficient of variation (CV) of $EPSP_1$ was carried out as previously described (Brock et al., 2020). Briefly, the locus of plasticity expression was determined by the angle φ between the diagonal and the CV endpoint. Presynaptic expression was indicated by $\varphi > 0$ at the $p < 0.05$ level as determined using a standard one-sample *t*-test, whereas postsynaptic expression was similarly indicated by $\varphi < 0$, whereas no significance would suggest a mixed pre- and postsynaptic locus of expression (Sjöström et al., 2007). CV analysis was only carried out with experiments showing at least 5% plasticity, meaning EPSP after/before > 105% for tLTP and EPSP after/before < 95% for tLTD.

Paired-pulse ratio (PPR) was calculated as $(EPSP_2 - EPSP_1)/EPSP_1$, taken from averages before and after tLTD induction. The change in PPR was calculated as $\Delta PPR = PPR_{after} - PPR_{before}$. A change in PPR after tLTD induction suggested altered probability of release, i.e., a presynaptic locus of expression (Sjöström et al., 2003).

As a clarification regarding the use of different baseline spiking pattern, we note that the presence of preNMDARs complicates the use of paired-pulse stimulation during baseline periods, since preNMDARs enhance release during high-frequency activity (Abrahamsson et al., 2017; Sjöström et al., 2003; Wong et al., 2024). Therefore, repeated stimulation can suppress synaptic responses when preNMDARs are blocked, potentially confounding interpretation. For this reason, we limited PPR analysis to Figures 5 and 6, where conditions were appropriate.

Pharmacology

MK-801 maleate (Hello Bio) and 7-CK (Alomone labs) were washed in at 2 mM and 100 µM, respectively (Nabavi et al., 2013; Sjöström et al., 2003), and slices were incubated for at least 30 minutes before the start of recordings. We used this high MK-801 concentration to match the mM-range concentrations commonly used intracellularly (Berretta and Jones, 1996;

Brasier and Feldman, 2008; Buchanan et al., 2012; Corlew et al., 2007; Larsen et al., 2011; Nevian and Sakmann, 2006; Rodríguez-Moreno et al., 2011; Rodríguez-Moreno and Paulsen, 2008), allowing a direct comparison of extra/intracellular MK-801 application. Lower extracellular MK-801 concentrations in the µM range (e.g., Huettner and Bean, 1988; Kemp et al., 1988; Tovar and Westbrook, 1999) were thus avoided to ensure robust NMDAR blockade and avoid false negatives due to incomplete inhibition. In JNK2 blockade experiments, slices were incubated in ACSF containing 4 µM SP600125 (Sigma-Aldrich) (Bennett et al., 2001) for at least 2 hours before the start of recordings. This concentration is specific for JNK2 over JNK1 and JNK3 (Abrahamsson et al., 2017; Nisticò et al., 2015).

The peptide used to selectively disrupt JNK2/STX1a interaction was synthesized by Université de Sherbrooke and corresponds to 12 residues (IEQSIEQEEGLNRS) that are part of the N-terminal amino acid sequence of STX1a interacting with JNK2 (Marcelli et al., 2019). Patch pipettes were loaded with 10 µM of the peptide. Neurons were patched for at least 30 minutes before tLTD induction.

Statistics

Unless stated otherwise, results are reported as the mean ± standard error of the mean, with n indicating number of connections. Boxplots show medians and quartiles, with whiskers denoting extremes. Significance levels are denoted using asterisks (*$p < 0.05$, **$p < 0.01$, ***$p < 0.001$). Pairwise comparisons were carried out using a two-tailed Student's *t*-test for equal means, unless otherwise indicated. If the equality of variances *F*-test gave $p < 0.05$, we employed the unequal variances *t*-test. Wilcoxon-Mann-Whitney's non-parametric test was used in parallel, with similar outcome to the *t*-test. Comparisons to a single value were done with a one-sample *t*-test, e.g., for CV analysis φ. Multiple comparisons were carried out using one-way ANOVA with Bonferroni's post-hoc correction. Pairwise comparisons were only made if ANOVA permitted it at the $p < 0.05$ level. Based on the outcome of Bartlett's test, we used homo- or heteroscedastic (Welch) ANOVA. Statistical tests were performed in Igor Pro and Prism 7.0 (GraphPad Software).

Acknowledgements

We thank Alanna Watt, Kim Dore, Airi Watanabe, and members of the Sjöström lab for help and useful discussions. We thank Marc-André Bonin for help with JGRi1 peptide synthesis.

Funding Statement

AT was supported by Marie Skłodowska-Curie fellowship 892837. SR was supported by doctoral awards from FRQS (317516), HBHL, and the RI-MUHC. JAB won Max Stern and IPN recruitment awards. HH-WW was supported by CIHR fellowship 295104, an HBHL postdoctoral fellowship, FRQS postdoctoral fellowship 259572, and QBIN scholarship 35450. PJS was a recipient of CFI LOF 28331, CIHR PG 156223, 191969, 191997, FRSQ CB 254033, NSERC DG/DAS 2024-06712, 2017-04730, 2017-507818, and Donald S. Wells Distinguished Scientist awards. The funders had no role in study design, data collection and interpretation, or the decision to submit the work for publication.

Conflict of Interest Statement:

The authors declare that the research was conducted in the absence of any commercial or financial relationships that could be construed as a potential conflict of interest.

Author Contribution

AT, SR, JAB, and HH-WW carried out experiments. AT, SR, and JAB performed analysis. PJS wrote custom software. AT and PJS wrote the manuscript with input from HH-WW and SR.

Data Availability Statement

The raw data supporting the conclusions of this manuscript is available from the authors.

References

Abrahamsson, T., Chou, C.Y.C., Li, S.Y., Mancino, A., Costa, R.P., Brock, J.A., Nuro, E., Buchanan, K.A., Elgar, D., Blackman, A.V., *et al.* 2017. Differential Regulation of Evoked and Spontaneous Release by Presynaptic NMDA Receptors. Neuron 96: 839-855.e835

Abrahamsson, T., Lalanne, T., Watt, A.J., and Sjöström, P.J. 2016. In Vitro Investigation of Synaptic Plasticity. Cold Spring Harb Protoc 2016: pdb.top087262

Aoki, C., Venkatesan, C., Go, C.G., Mong, J.A., and Dawson, T.M. 1994. Cellular and subcellular localization of NMDA-R1 subunit immunoreactivity in the visual cortex of adult and neonatal rats. J Neurosci 14: 5202-5222.

Banerjee, A., Gonzalez-Rueda, A., Sampaio-Baptista, C., Paulsen, O., and Rodríguez-Moreno, A. 2014. Distinct mechanisms of spike timing-dependent LTD at vertical and horizontal inputs onto L2/3 pyramidal neurons in mouse barrel cortex. Physiological reports 2: e00271

Banerjee, A., Meredith, R.M., Rodríguez-Moreno, A., Mierau, S.B., Auberson, Y.P., and Paulsen, O. 2009. Double Dissociation of Spike Timing-Dependent Potentiation and Depression by Subunit-Preferring NMDA Receptor Antagonists in Mouse Barrel Cortex. Cereb Cortex

Bartlett, R.D., Esslinger, C.S., Thompson, C.M., and Bridges, R.J. 1998. Substituted quinolines as inhibitors of L-glutamate transport into synaptic vesicles. Neuropharmacology 37: 839-846

Bender, V.A., Bender, K.J., Brasier, D.J., and Feldman, D.E. 2006. Two coincidence detectors for spike timing-dependent plasticity in somatosensory cortex. J Neurosci 26: 4166-4177

Bennett, B.L., Sasaki, D.T., Murray, B.W., O'Leary, E.C., Sakata, S.T., Xu, W., Leisten, J.C., Motiwala, A., Pierce, S., Satoh, Y., *et al.* 2001. SP600125, an anthrapyrazolone inhibitor of Jun N-terminal kinase. PNAS 98: 13681-13686

Berretta, N., and Jones, R.S. 1996. Tonic facilitation of glutamate release by presynaptic N-methyl-D-aspartate autoreceptors in the entorhinal cortex. Neuroscience 75: 339-344.

Bi, G.Q., and Poo, M.M. 1998. Synaptic modifications in cultured hippocampal neurons: dependence on spike timing, synaptic strength, and postsynaptic cell type. Journal of Neuroscience 18: 10464-10472

Bidoret, C., Ayon, A., Barbour, B., and Casado, M. 2009. Presynaptic NR2A-containing NMDA receptors implement a high-pass filter synaptic plasticity rule. PNAS 106: 14126-14131

Blackman, A.V., Grabuschnig, S., Legenstein, R., and Sjöström, P.J. 2014. A comparison of manual neuronal reconstruction from biocytin histology or 2-photon imaging: morphometry and computer modeling. Front Neuroanat 8: 65

Bliss, T.V., and Collingridge, G.L. 1993. A synaptic model of memory: long-term potentiation in the hippocampus. Nature 361: 31-39

Bouvier, G., Larsen, R.S., Rodriguez-Moreno, A., Paulsen, O., and Sjöström, P.J. 2018. Towards resolving the presynaptic NMDA receptor debate. Curr Opin Neurobiol 51: 1-7

Brasier, D.J., and Feldman, D.E. 2008. Synapse-specific expression of functional presynaptic NMDA receptors in rat somatosensory cortex. J Neurosci 28: 2199-2211

Brock, J.A., Thomazeau, A., Watanabe, A., Li, S.S.Y., and Sjöström, P.J. 2020. A Practical Guide to Using CV Analysis for Determining the Locus of Synaptic Plasticity. Front Synaptic Neurosci 12: 11

Buchanan, K.A., Blackman, A.V., Moreau, A.W., Elgar, D., Costa, R.P., Lalanne, T., Tudor Jones, A.A., Oyrer, J., and Sjöström, P.J. 2012. Target-Specific Expression of Presynaptic NMDA Receptors in Neocortical Microcircuits. Neuron 75: 451-466

Carter, B.C., and Jahr, C.E. 2016. Postsynaptic, not presynaptic NMDA receptors are required for spike-timing-dependent LTD induction. Nat Neurosci 19: 1218-1224

Casado, M., Dieudonne, S., and Ascher, P. 2000. Presynaptic N-methyl-D-aspartate receptors at the parallel fiber-Purkinje cell synapse. PNAS 97: 11593-11597.

Casado, M., Isope, P., and Ascher, P. 2002. Involvement of presynaptic N-methyl-D-aspartate receptors in cerebellar long-term depression. Neuron 33: 123-130.

Castillo, P.E., Schoch, S., Schmitz, F., Südhof, T.C., and Malenka, R.C. 2002. RIM1alpha is required for presynaptic long-term potentiation. Nature 415: 327-330

Castillo, P.E., Younts, T.J., Chavez, A.E., and Hashimotodani, Y. 2012. Endocannabinoid signaling and synaptic function. Neuron 76: 70-81

Chevaleyre, V., Heifets, B.D., Kaeser, P.S., Südhof, T.C., and Castillo, P.E. 2007. Endocannabinoid-mediated long-term plasticity requires cAMP/PKA signaling and RIM1alpha. Neuron 54: 801-812

Chou, C.Y.C., Wong, H.H.W., Guo, C., Boukoulou, K.E., Huang, C., Jannat, J., Klimenko, T., Li, V.Y., Liang, T.A., Wu, V.C., and Sjöström, P.J. 2024. Principles of visual cortex excitatory microcircuit organization. The Innovation 6: 1-11

Christie, J.M., and Jahr, C.E. 2008. Dendritic NMDA receptors activate axonal calcium channels. Neuron 60: 298-307

Christie, J.M., and Jahr, C.E. 2009. Selective expression of ligand-gated ion channels in L5 pyramidal cell axons. J Neurosci 29: 11441-11450

Cline, H.T. 1998. Topographic maps: developing roles of synaptic plasticity. Curr Biol 8: R836-839

Coffey, E.T. 2014. Nuclear and cytosolic JNK signalling in neurons. Nat Rev Neurosci 15: 285-299

Corlew, R., Wang, Y., Ghermazien, H., Erisir, A., and Philpot, B.D. 2007. Developmental switch in the contribution of presynaptic and postsynaptic NMDA receptors to long-term depression. J Neurosci 27: 9835-9845

Curran, B.P., Murray, H.J., and O'Connor, J.J. 2003. A role for c-Jun N-terminal kinase in the inhibition of long-term potentiation by interleukin-1beta and long-term depression in the rat dentate gyrus in vitro. Neuroscience 118: 347-357

Debanne, D., and Inglebert, Y. 2023. Spike timing-dependent plasticity and memory. Curr Opin Neurobiol 80: 102707

DeBiasi, S., Minelli, A., Melone, M., and Conti, F. 1996. Presynaptic NMDA receptors in the neocortex are both auto- and heteroreceptors. Neuroreport 7: 2773-2776.

Dore, K., Stein, I.S., Brock, J.A., Castillo, P.E., Zito, K., and Sjöström, P.J. 2017. Unconventional NMDA Receptor Signaling. J Neurosci 37: 10800-10807

Duguid, I., and Sjöström, P.J. 2006. Novel presynaptic mechanisms for coincidence detection in synaptic plasticity. Curr Opin Neurobiol 16: 312-322

Feldman, D.E. 2000. Timing-based LTP and LTD at vertical inputs to layer II/III pyramidal cells in rat barrel cortex. Neuron 27: 45-56

Feldman, D.E. 2012. The spike-timing dependence of plasticity. Neuron 75: 556-571

Fourcaudot, E., Gambino, F., Humeau, Y., Casassus, G., Shaban, H., Poulain, B., and Luthi, A. 2008. cAMP/PKA signaling and RIM1alpha mediate presynaptic LTP in the lateral amygdala. PNAS 105: 15130-15135

Foust, K.D., Nurre, E., Montgomery, C.L., Hernandez, A., Chan, C.M., and Kaspar, B.K. 2009. Intravascular AAV9 preferentially targets neonatal neurons and adult astrocytes. Nat Biotechnol 27: 59-65

Glitsch, M., and Marty, A. 1999. Presynaptic effects of NMDA in cerebellar Purkinje cells and interneurons. J Neurosci 19: 511-519.

Gorski, J.A., Talley, T., Qiu, M., Puelles, L., Rubenstein, J.L., and Jones, K.R. 2002. Cortical excitatory neurons and glia, but not GABAergic neurons, are produced in the Emx1-expressing lineage. J Neurosci 22: 6309-6314

Hebb, D.O. 1949. The Organization of Behavior (New York: Wiley)

Heinbockel, T., Brager, D.H., Reich, C.G., Zhao, J., Muralidharan, S., Alger, B.E., and Kao, J.P. 2005. Endocannabinoid signaling dynamics probed with optical tools. J Neurosci 25: 9449-9459

Heuss, C., and Gerber, U. 2000. G-protein-independent signaling by G-protein-coupled receptors. Trends in Neurosciences 23: 469-475

Hioki, H., Kameda, H., Nakamura, H., Okunomiya, T., Ohira, K., Nakamura, K., Kuroda, M., Furuta, T., and Kaneko, T. 2007. Efficient gene transduction of neurons by lentivirus with enhanced neuron-specific promoters. Gene Ther 14: 872-882

Huettner, J.E., and Bean, B.P. 1988. Block of N-methyl-D-aspartate-activated current by the anticonvulsant MK-801: selective binding to open channels. PNAS 85: 1307-1311.

Kaeser, P.S., Kwon, H.B., Chiu, C.Q., Deng, L., Castillo, P.E., and Südhof, T.C. 2008. RIM1alpha and RIM1beta are synthesized from distinct promoters of the RIM1 gene to mediate differential but overlapping synaptic functions. J Neurosci 28: 13435-13447

Katz, L.C., and Shatz, C.J. 1996. Synaptic activity and the construction of cortical circuits. Science 274: 1133-1138

Kemp, J.A., Foster, A.C., Leeson, P.D., Priestley, T., Tridgett, R., Iversen, L.L., and Woodruff, G.N. 1988. 7-Chlorokynurenic acid is a selective antagonist at the glycine modulatory site of the N-methyl-D-aspartate receptor complex. PNAS 85: 6547-6550

Kim, J.Y., Grunke, S.D., Levites, Y., Golde, T.E., and Jankowsky, J.L. 2014. Intracerebroventricular viral injection of the neonatal mouse brain for persistent and widespread neuronal transduction. Journal of visualized experiments : JoVE: 51863

Klein, R., Ruttkowski, B., Knapp, E., Salmons, B., Günzburg, W.H., and Hohenadl, C. 2006. WPRE-mediated enhancement of gene expression is promoter and cell line specific. Gene 372: 153-161

Koester, H.J., and Sakmann, B. 1998. Calcium dynamics in single spines during coincident pre- and postsynaptic activity depend on relative timing of back-propagating action potentials and subthreshold excitatory postsynaptic potentials. PNAS 95: 9596-9601

Kunz, P.A., Roberts, A.C., and Philpot, B.D. 2013. Presynaptic NMDA receptor mechanisms for enhancing spontaneous neurotransmitter release. J Neurosci 33: 7762-7769

Lalanne, T., Abrahamsson, T., and Sjöström, P.J. 2016. Using Multiple Whole-Cell Recordings to Study Spike-Timing-Dependent Plasticity in Acute Neocortical Slices. Cold Spring Harb Protoc 2016: pdb.prot091306

Larsen, R.S., Corlew, R.J., Henson, M.A., Roberts, A.C., Mishina, M., Watanabe, M., Lipton, S.A., Nakanishi, N., Perez-Otano, I., Weinberg, R.J., and Philpot, B.D. 2011. NR3A-containing NMDARs promote neurotransmitter release and spike timing-dependent plasticity. Nat Neurosci 14: 338-344

Larsen, R.S., and Sjöström, P.J. 2015. Synapse-type-specific plasticity in local circuits. Curr Opin Neurobiol 35: 127-135

Larsen, R.S., Smith, I.T., Miriyala, J., Han, J.E., Corlew, R.J., Smith, S.L., and Philpot, B.D. 2014. Synapse-specific control of experience-dependent plasticity by presynaptic NMDA receptors. Neuron 83: 879-893

Lisman, J.E., Coyle, J.T., Green, R.W., Javitt, D.C., Benes, F.M., Heckers, S., and Grace, A.A. 2008. Circuit-based framework for understanding neurotransmitter and risk gene interactions in schizophrenia. Trends Neurosci 31: 234-242

Liu, H., Mantyh, P.W., and Basbaum, A.I. 1997. NMDA-receptor regulation of substance P release from primary afferent nociceptors. Nature 386: 721-724.

Liu, Z., Chen, O., Wall, J.B.J., Zheng, M., Zhou, Y., Wang, L., Vaseghi, H.R., Qian, L., and Liu, J. 2017. Systematic comparison of 2A peptides for cloning multi-genes in a polycistronic vector. Sci Rep 7: 2193

Malenka, R.C., and Bear, M.F. 2004. LTP and LTD: an embarrassment of riches. Neuron 44: 5-21

Marcelli, S., Iannuzzi, F., Ficulle, E., Mango, D., Pieraccini, S., Pellegrino, S., Corbo, M., Sironi, M., Pittaluga, A., Nistico, R., and Feligioni, M. 2019. The selective disruption of presynaptic JNK2/STX1a interaction reduces NMDA receptor-dependent glutamate release. Sci Rep 9: 7146

Markram, H., Gerstner, W., and Sjöström, P.J., eds. (2012). Spike-timing-dependent plasticity: a comprehensive overview. (Lausanne, Switzerland: Frontiers Media SA).

Markram, H., Lübke, J., Frotscher, M., and Sakmann, B. 1997. Regulation of synaptic efficacy by coincidence of postsynaptic APs and EPSPs. Science 275: 213-215

Martínez-Gallego, I., Pérez-Rodríguez, M., Coatl-Cuaya, H., Flores, G., and Rodríguez-Moreno, A. 2022. Adenosine and Astrocytes Determine the Developmental Dynamics of Spike Timing-Dependent Plasticity in the Somatosensory Cortex. J Neurosci 42: 6038-6052

McFarlan, A.R., Chou, C.Y.C., Watanabe, A., Cherepacha, N., Haddad, M., Owens, H., and Sjöström, P.J. 2023. The plasticitome of cortical interneurons. Nat Rev Neurosci 24: 80-97

McGuinness, L., Taylor, C., Taylor, R.D., Yau, C., Langenhan, T., Hart, M.L., Christian, H., Tynan, P.W., Donnelly, P., and Emptage, N.J. 2010. Presynaptic NMDARs in the hippocampus facilitate transmitter release at theta frequency. Neuron 68: 1109-1127

Mittelstaedt, T., Alvarez-Baron, E., and Schoch, S. 2010. RIM proteins and their role in synapse function. Biol Chem 391: 599-606

Morel, C., Sherrin, T., Kennedy, N.J., Forest, K.H., Avcioglu Barutcu, S., Robles, M., Carpenter-Hyland, E., Alfulaij, N., Standen, C.L., Nichols, R.A., *et al.* 2018. JIP1-Mediated JNK Activation Negatively Regulates Synaptic Plasticity and Spatial Memory. J Neurosci 38: 3708-3728

Mukherjee, P.K., DeCoster, M.A., Campbell, F.Z., Davis, R.J., and Bazan, N.G. 1999. Glutamate receptor signaling interplay modulates stress-sensitive mitogen-activated protein kinases and neuronal cell death. J Biol Chem 274: 6493-6498

Nabavi, S., Fox, R., Proulx, C.D., Lin, J.Y., Tsien, R.Y., and Malinow, R. 2014. Engineering a memory with LTD and LTP. Nature 511: 348-352

Nabavi, S., Kessels, H.W., Alfonso, S., Aow, J., Fox, R., and Malinow, R. 2013. Metabotropic NMDA receptor function is required for NMDA receptor-dependent long-term depression. PNAS 110: 4027-4032

Nagy, A. 2000. Cre recombinase: the universal reagent for genome tailoring. Genesis 26: 99-109

Nevian, T., and Sakmann, B. 2006. Spine Ca^{2+} signaling in spike-timing-dependent plasticity. J Neurosci 26: 11001-11013

Nielsen, A.C., Anderson, C.L., Ens, C., Boyce, A.K.J., and Thompson, R.J. 2024. Non-ionotropic NMDAR signalling activates Panx1 to induce P2X4R-dependent long-term depression in the hippocampus. J Physiol

Nisticò, R., Florenzano, F., Mango, D., Ferraina, C., Grilli, M., Di Prisco, S., Nobili, A., Saccucci, S., D'Amelio, M., Morbin, M., *et al.* 2015. Presynaptic c-Jun N-terminal Kinase 2 regulates NMDA receptor-dependent glutamate release. Sci Rep 5: 9035

Nugent, F.S., Kirkwood, A., Lupica, C.R., and Sjöström, P.J. 2022. The synaptic basis of neuropathology. Frontiers in Synaptic Neuroscience 14

Paoletti, P., Bellone, C., and Zhou, Q. 2013. NMDA receptor subunit diversity: impact on receptor properties, synaptic plasticity and disease. Nat Rev Neurosci 14: 383-400

Park, D.K., Stein, I.S., and Zito, K. 2022. Ion flux-independent NMDA receptor signaling. Neuropharmacology 210: 109019

Rodríguez-Moreno, A., Gonzalez-Rueda, A., Banerjee, A., Upton, A.L., Craig, M.T., and Paulsen, O. 2013. Presynaptic self-depression at developing neocortical synapses. Neuron 77: 35-42

Rodríguez-Moreno, A., Kohl, M.M., Reeve, J.E., Eaton, T.R., Collins, H.A., Anderson, H.L., and Paulsen, O. 2011. Presynaptic induction and expression of timing-dependent long-term depression demonstrated by compartment-specific photorelease of a use-dependent NMDA receptor antagonist. J Neurosci 31: 8564-8569

Rodriguez-Moreno, A., and Lerma, J. 1998. Kainate receptor modulation of GABA release involves a metabotropic function. Neuron 20: 1211-1218

Rodríguez-Moreno, A., and Paulsen, O. 2008. Spike timing-dependent long-term depression requires presynaptic NMDA receptors. Nat Neurosci 11: 744-745

Rueda, D., Galve-Roperh, I., Haro, A., and Guzmán, M. 2000. The CB(1) cannabinoid receptor is coupled to the activation of c-Jun N-terminal kinase. Mol Pharmacol 58: 814-820

Sjöström, P.J., and Nelson, S.B. 2002. Spike timing, calcium signals and synaptic plasticity. Curr Opin Neurobiol 12: 305-314.

Sjöström, P.J., Turrigiano, G.G., and Nelson, S.B. 2001. Rate, timing, and cooperativity jointly determine cortical synaptic plasticity. Neuron 32: 1149-1164

Sjöström, P.J., Turrigiano, G.G., and Nelson, S.B. 2003. Neocortical LTD via coincident activation of presynaptic NMDA and cannabinoid receptors. Neuron 39: 641-654

Sjöström, P.J., Turrigiano, G.G., and Nelson, S.B. 2007. Multiple forms of long-term plasticity at unitary neocortical layer 5 synapses. Neuropharmacology 52: 176-184

Song, S., and Abbott, L.F. 2001. Cortical development and remapping through spike timing-dependent plasticity. Neuron 32: 339-350

Song, S., Sjöström, P.J., Reigl, M., Nelson, S., and Chklovskii, D.B. 2005. Highly nonrandom features of synaptic connectivity in local cortical circuits. PLoS biology 3: e68

Song, X., Jensen, M.O., Jogini, V., Stein, R.A., Lee, C.H., McHaourab, H.S., Shaw, D.E., and Gouaux, E. 2018. Mechanism of NMDA receptor channel block by MK-801 and memantine. Nature 556: 515-519

Stein, I.S., Park, D.K., Claiborne, N., and Zito, K. 2021. Non-ionotropic NMDA receptor signaling gates bidirectional structural plasticity of dendritic spines. Cell Rep 34: 108664

Stuart, G.J., and Sakmann, B. 1994. Active propagation of somatic action potentials into neocortical pyramidal cell dendrites. Nature 367: 69-72

Takago, H., Nakamura, Y., and Takahashi, T. 2005. G protein-dependent presynaptic inhibition mediated by AMPA receptors at the calyx of Held. PNAS 102: 7368-7373

Thomazeau, A., Bosch, M., Essayan-Perez, S., Barnes, S.A., De Jesus-Cortes, H., and Bear, M.F. 2021. Dissociation of functional and structural plasticity of dendritic spines during NMDAR and mGluR-dependent long-term synaptic depression in wild-type and fragile X model mice. Mol Psychiatry 26: 4652-4669

Tovar, K.R., and Westbrook, G.L. 1999. The incorporation of NMDA receptors with a distinct subunit composition at nascent hippocampal synapses in vitro. J Neurosci 19: 4180-4188

Trus, M., and Atlas, D. 2024. Non-ionotropic voltage-gated calcium channel signaling. Channels (Austin) 18: 2341077

Wang, Y., and Durkin, J.P. 1995. alpha-Amino-3-hydroxy-5-methyl-4-isoxazolepropionic acid, but not N-methyl-D-aspartate, activates mitogen-activated protein kinase through G-protein beta gamma subunits in rat cortical neurons. J Biol Chem 270: 22783-22787

Watanabe, A., Guo, C., and Sjostrom, P.J. 2023. The developmental profile of visual cortex astrocytes. iScience 26: 106828

Weilinger, N.L., Lohman, A.W., Rakai, B.D., Ma, E.M., Bialecki, J., Maslieieva, V., Rilea, T., Bandet, M.V., Ikuta, N.T., Scott, L., *et al.* 2016. Metabotropic NMDA receptor signaling couples Src family kinases to pannexin-1 during excitotoxicity. Nat Neurosci 19: 432-442

Wong, H.H., Rannio, S., Jones, V., Thomazeau, A., and Sjöström, P.J. 2021. NMDA receptors in axons: there's no coincidence. J Physiol 599: 367-387

Wong, H.H., Watt, A.J., and Sjöström, P.J. 2024. Synapse-specific burst coding sustained by local axonal translation. Neuron 112: 264-276 e266

Yamasaki, T., Kawasaki, H., and Nishina, H. 2012. Diverse Roles of JNK and MKK Pathways in the Brain. J Signal Transduct 2012: 459265

Yuste, R., and Denk, W. 1995. Dendritic spines as basic functional units of neuronal integration. Nature 375: 682-684

Zhang, L.I., Tao, H.W., Holt, C.E., Harris, W.A., and Poo, M. 1998. A critical window for cooperation and competition among developing retinotectal synapses. Nature 395: 37-44

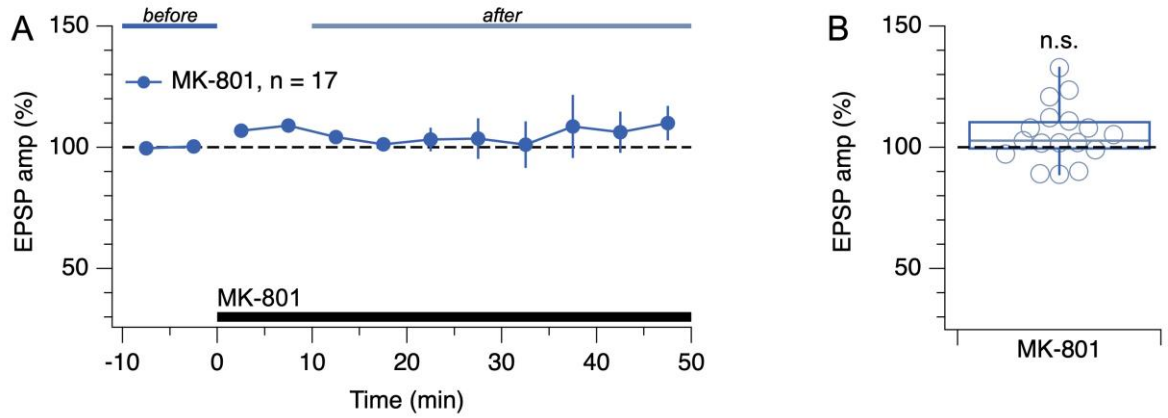

Supplementary Figure 1. Low-frequency evoked release did not respond to MK-801.

(A, B) Washing in MK-801 had no appreciable effect on EPSP amplitude (one-sample *t*-test for normalized EPSP vs. 100%, p = 0.076). Presynaptic cells spiked once every 10 seconds. This outcome is consistent with the finding that preNMDAR activation requires firing above a critical frequency (Abrahamsson et al., 2017; Buchanan et al., 2012; Sjöström et al., 2003; Wong et al., 2024). Before (blue) and after lines (light blue) indicate periods used for EPSP normalization.

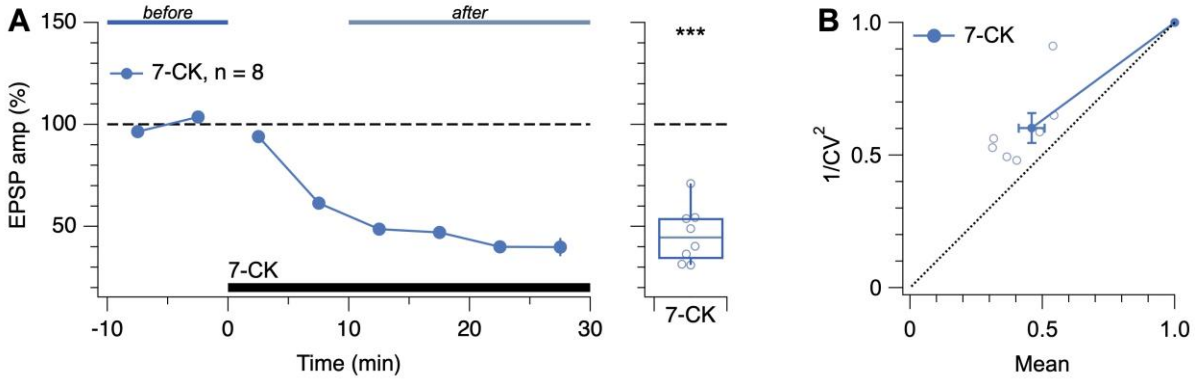

Supplementary Figure 2. Low-frequency evoked release was suppressed by 7-CK.

(A) Washing in 7-CK drastically reduced EPSP amplitude (one-sample *t*-test for normalized EPSP vs. 100%, p < 0.001). Presynaptic cells spiked once every 10 seconds. Experiments with 7-CK (**Figure 4**) therefore required waiting for responses to asymptotically stabilize. Blue and light-blue lines indicate periods used for quantification of EPSP amplitude.

(B) CV analysis of the 7-CK-mediated suppression gave rise to data points above the diagonal (φ = -11º ± 4º, n = 7, p < 0.05), suggesting reduced quantal amplitude (Brock et al., 2020). This outcome is consistent with 7-CK also acting as a competitive inhibitor of L-glutamate transport into synaptic vesicles (Bartlett et al., 1998), so that after 7-CK, vesicles may contain less neurotransmitter. However, $1/CV^2$ was also decreased (after/before = 0.6 ± 0.06, n = 7, one-sample *t*-test vs. 1, p < 0.001), suggesting that $p_{release}$ was simultaneously reduced (Brock et al., 2020).

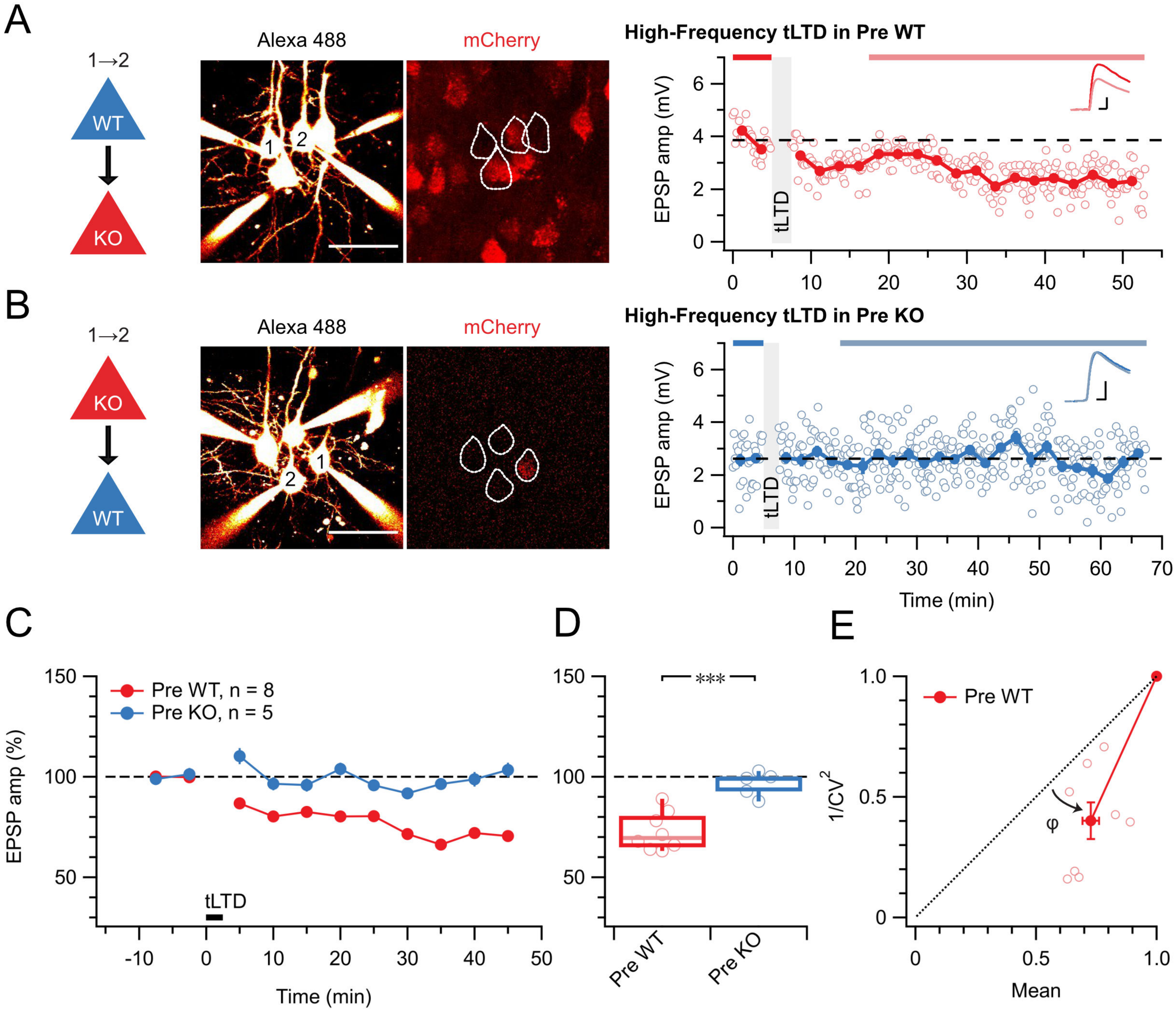
A
1→2
WT
KO
Alexa 488
mCherry
1
2
High-Frequency tLTD in Pre WT
EPSP amp (mV)
tLTD
B
1→2
KO
WT
High-Frequency tLTD in Pre KO
Time (min)
C
Pre WT, n = 8
Pre KO, n = 5
EPSP amp (%)
tLTD
Time (min)
D
***
Pre WT
Pre KO
E
Pre WT
1/CV²
φ
Mean

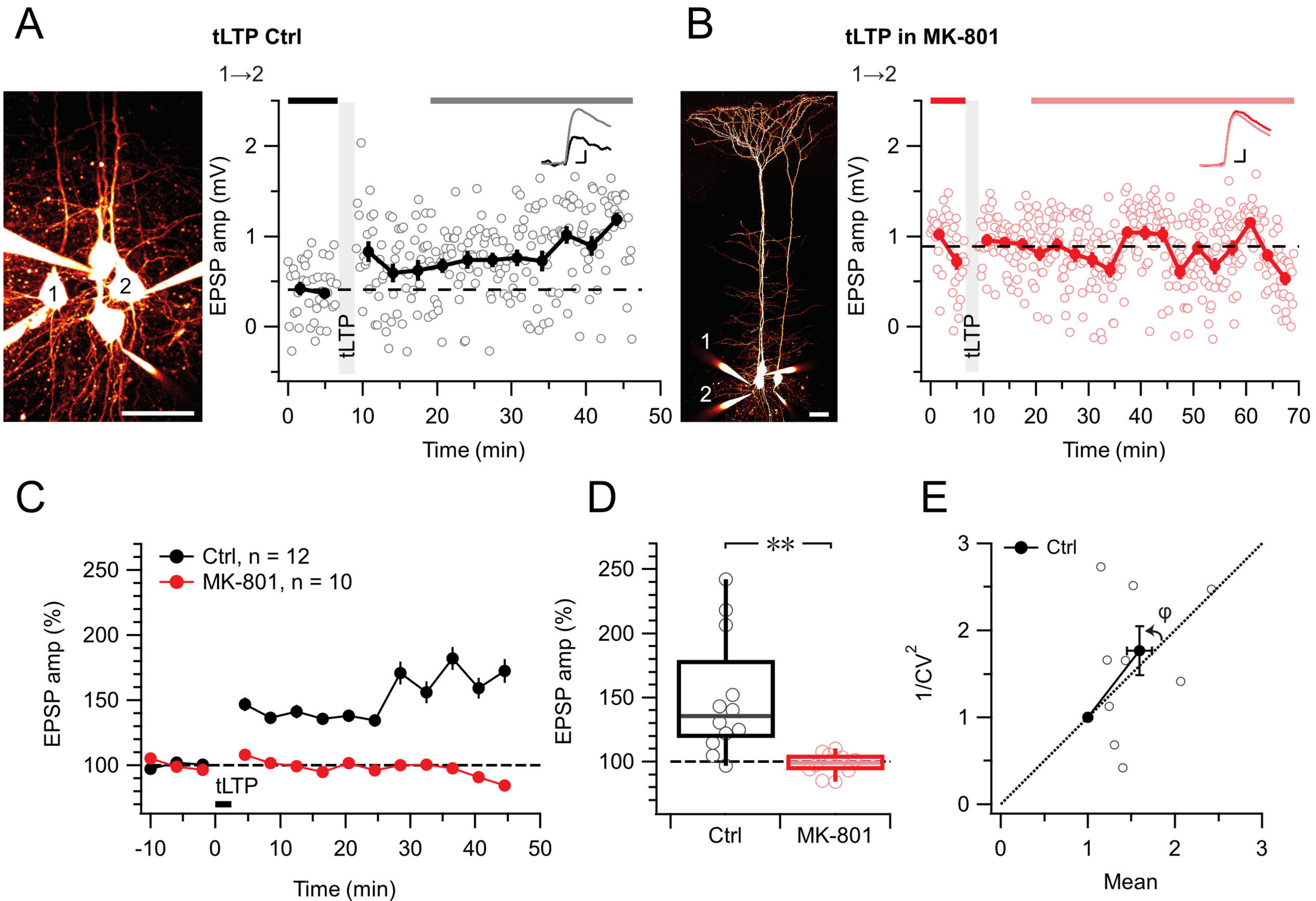
A
tLTP Ctrl
1→2
EPSP amp (mV)
tLTP
Time (min)
B
tLTP in MK-801
1→2
EPSP amp (mV)
tLTP
Time (min)
C
Ctrl, n = 12
MK-801, n = 10
EPSP amp (%)
tLTP
Time (min)
D
**
EPSP amp (%)
Ctrl
MK-801
E
Ctrl
φ
1/CV²
Mean

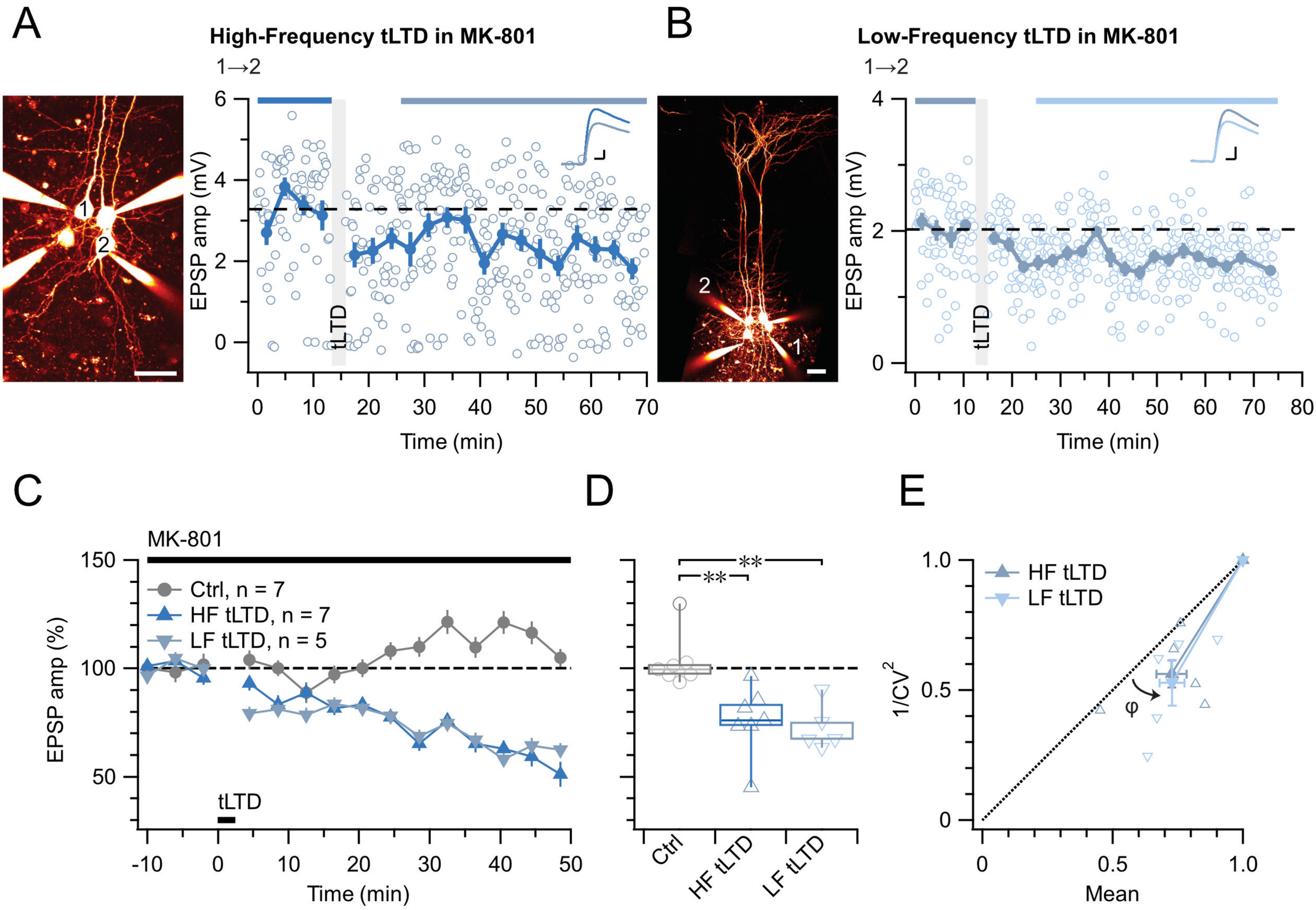
A
High-Frequency tLTD in MK-801
1→2
EPSP amp (mV)
tLTD
Time (min)
B
Low-Frequency tLTD in MK-801
1→2
EPSP amp (mV)
tLTD
Time (min)
C
MK-801
Ctrl, n = 7
HF tLTD, n = 7
LF tLTD, n = 5
EPSP amp (%)
tLTD
Time (min)
D
**
**
Ctrl
HF tLTD
LF tLTD
E
HF tLTD
LF tLTD
1/CV²
φ
Mean

A

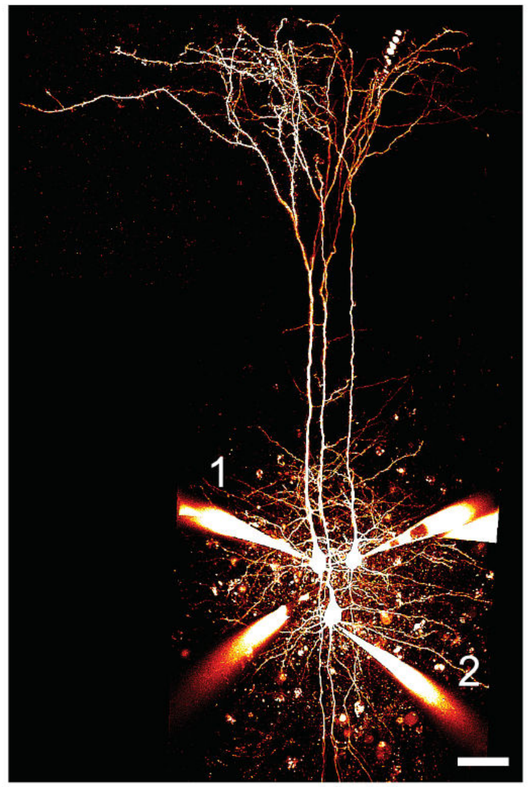
1
2

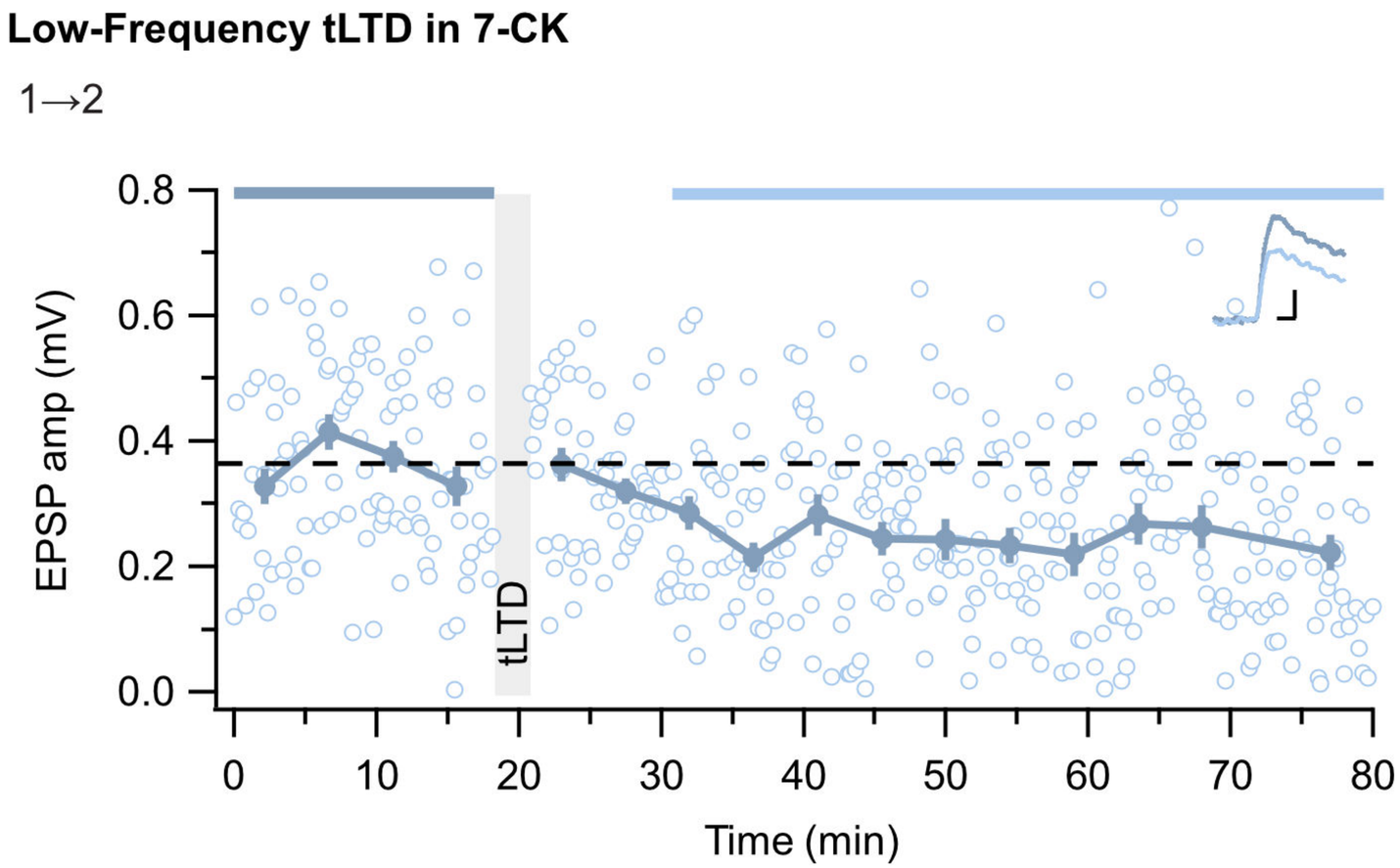
Low-Frequency tLTD in 7-CK
1→2
EPSP amp (mV)
0.8
0.6
0.4
0.2
0.0
tLTD
0
10
20
30
40
50
60
70
80
Time (min)

B

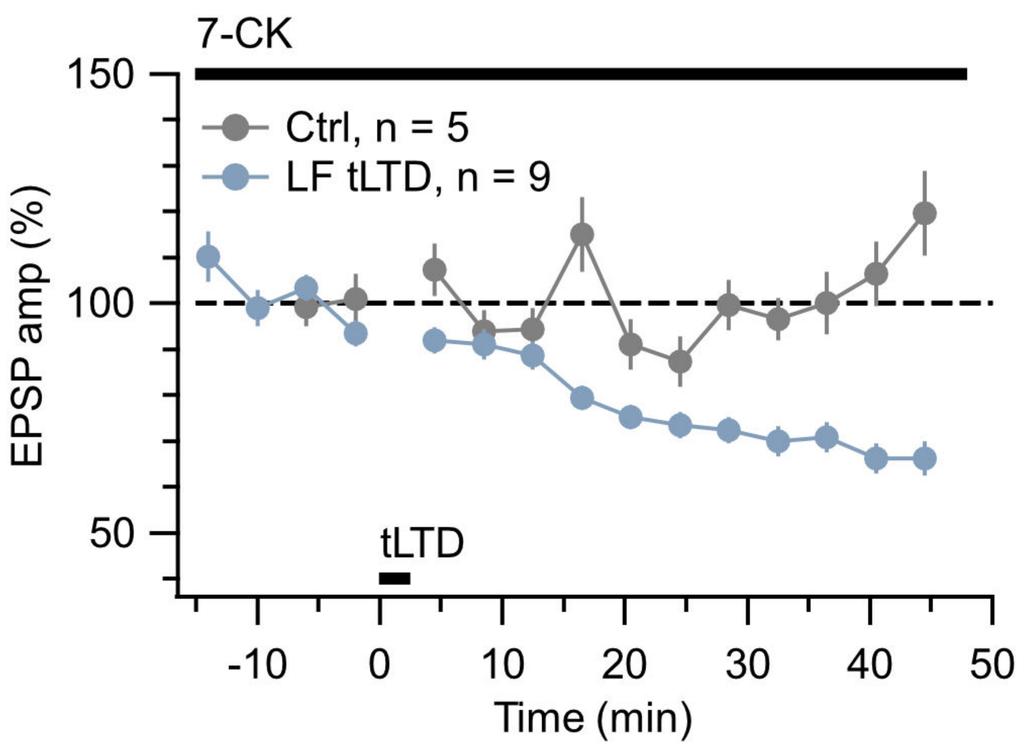
7-CK
Ctrl, n = 5
LF tLTD, n = 9
EPSP amp (%)
150
100
50
tLTD
-10
0
10
20
30
40
50
Time (min)

C

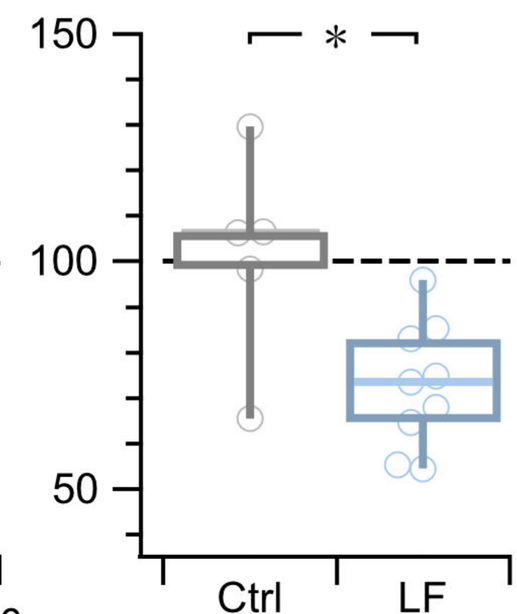
150
100
50
*
Ctrl
LF

D

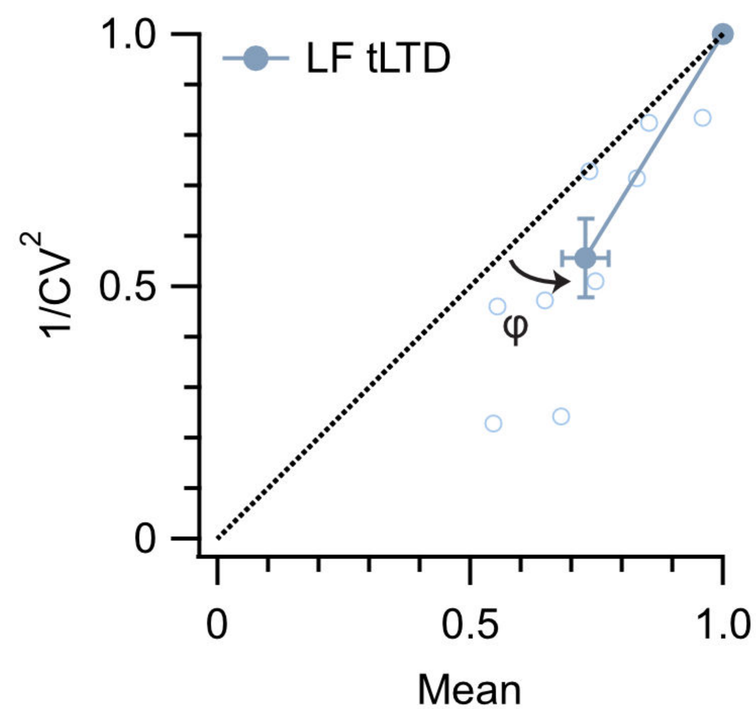
LF tLTD
1/CV²
1.0
0.5
0
φ
0
0.5
1.0
Mean

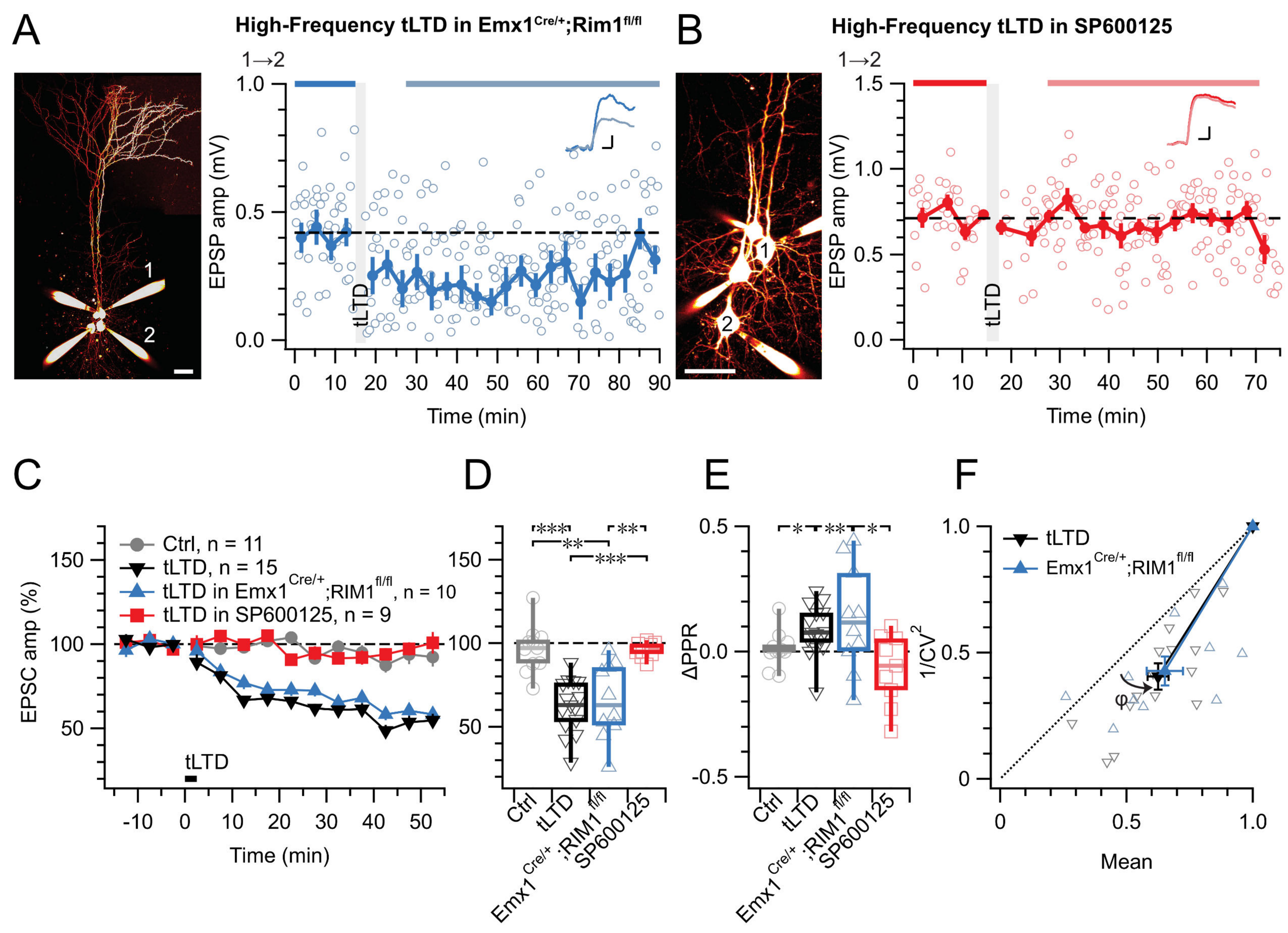
A
High-Frequency tLTD in Emx1Cre/+;Rim1fl/fl
1→2
EPSP amp (mV)
tLTD
Time (min)
B
High-Frequency tLTD in SP600125
1→2
EPSP amp (mV)
tLTD
Time (min)
C
Ctrl, n = 11
tLTD, n = 15
tLTD in Emx1Cre/+;RIM1fl/fl, n = 10
tLTD in SP600125, n = 9
EPSC amp (%)
tLTD
Time (min)
D
ΔPPR
Ctrl
tLTD
Emx1Cre/+;RIM1fl/fl
SP600125
E
1/CV2
Ctrl
tLTD
Emx1Cre/+;RIM1fl/fl
SP600125
F
tLTD
Emx1Cre/+;RIM1fl/fl
φ
Mean

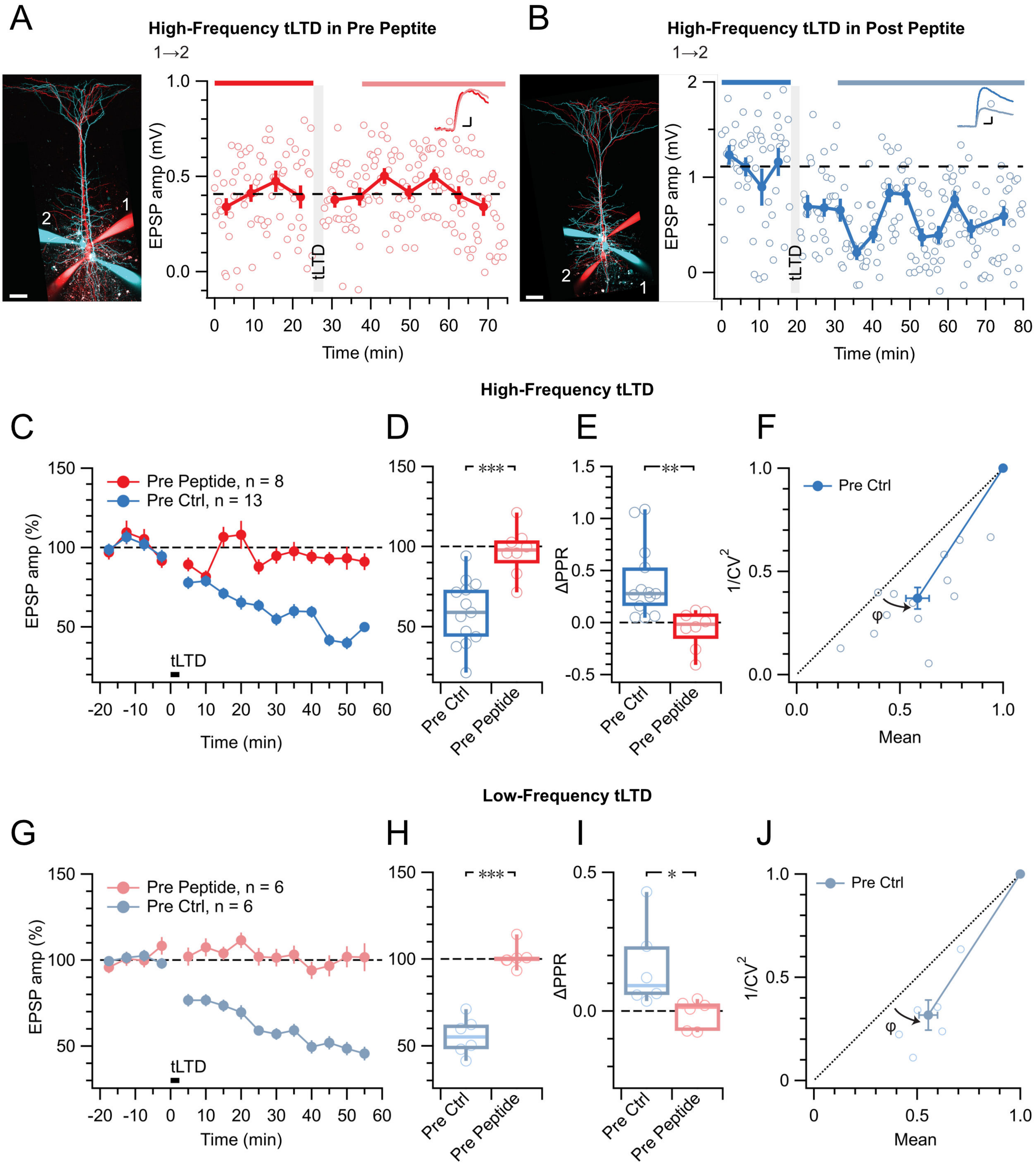
A
High-Frequency tLTD in Pre Peptite
1→2
EPSP amp (mV)
tLTD
Time (min)
B
High-Frequency tLTD in Post Peptite
1→2
EPSP amp (mV)
tLTD
Time (min)
High-Frequency tLTD
C
Pre Peptide, n = 8
Pre Ctrl, n = 13
EPSP amp (%)
tLTD
Time (min)
D
***
Pre Ctrl
Pre Peptide
E
**
ΔPPR
Pre Ctrl
Pre Peptide
F
Pre Ctrl
1/CV²
φ
Mean
Low-Frequency tLTD
G
Pre Peptide, n = 6
Pre Ctrl, n = 6
EPSP amp (%)
tLTD
Time (min)
H
***
Pre Ctrl
Pre Peptide
I
*
ΔPPR
Pre Ctrl
Pre Peptide
J
Pre Ctrl
1/CV²
φ
Mean